European Journal of Pharmaceutical Sciences

Identification of Novel SIRT1 Activators Endowed with Cardioprotective Profile

--Manuscript Draft--

Manuscript Number:	PHASCI-D-21-00589R1
Article Type:	Research Paper
Keywords:	SIRT1 activators; epigenetics; cardioprotection; computer-aided drug discovery; organic synthesis; pyrido[1,2-a]pyrimidin-4-ones; imidazo[1,2-a]pyridines.
Corresponding Author:	simone brogi, PhD University of Pisa: Universita degli Studi di Pisa Pisa, Toscana ITALY
First Author:	Lorenzo Flori
Order of Authors:	Lorenzo Flori
	Giovanni Petrarolo
	simone brogi, PhD
	Concettina La Motta
	Lara Testai
	Vincenzo Calderone
Manuscript Region of Origin:	ITALY
Abstract:	Drugs targeting epigenetic mechanisms are attracting the attention of scientists since it was observed that the modulation of this post-translational apparatus, could help to identify innovative therapeutic strategies. Among the epigenetic druggable targets, the positive modulation of SIRT1 has also been related to significant cardioprotective effects. Unfortunately, actual SIRT1 activators (natural products and synthetic molecules) suffer from several drawbacks, particularly poor pharmacokinetic profiles. Accordingly, in this article we present the development of an integrated screening platform aimed at identifying novel SIRT1 activators with favorable drug-like features as cardioprotective agents. Encompassing several competencies (in silico , medicinal chemistry, and pharmacology), we describe a multidisciplinary approach for rapidly identifying SIRT1 activators and their preliminary pharmacological characterization. In the first step, we virtually screened an in-house chemical library comprising synthetic molecules inspired by nature, against SIRT1 enzyme. To this end, we combined molecular docking-based approach with the estimation of relative ligand binding energy, using the crystal structure of SIRT1 enzyme in complex with resveratrol. Eleven computational hits were identified synthesized and tested against the isolated enzyme for validating the in silico strategy. Among the tested molecules, five of them behave as SIRT1 enzyme activators. Due to the superior response in activating the enzyme and its favorable calculated physico-chemical properties, compound 8 was further characterized in ex vivo studies on isolated and perfused rat hearts submitted to ischemia/reperfusion (I/R) period. The pharmacological profile of compound 8 , suggests that this molecule represents a prototypic SIRT1 activator with satisfactory drug-like profile, paving the way for developing novel epigenetic cardioprotective agents.

UNIVERSITÀ DI PISA
codice fiscale 80003670504
partita IVA 00286820501

DIPARTIMENTO DI FARMACIA
Via Bonanno, 6 - 56126 Pisa (Italy)
tel. 0039 050 2219500 - 510 - 545
fax 0039 050 2219608
Direttore: Prof.ssa Maria Letizia Trincavelli

DIPARTIMENTO FARMACIA
www.farm.unipi.it

June 16th, 2021

RE: Submission of the revised version of the manuscript quoted PHASCI-D-21-00589 "**Identification of Novel SIRT1 Activators Endowed with Cardioprotective Profile**" as a research article for publication in the "European Journal of Pharmaceutical Sciences", authored by Lorenzo Flori, Giovanni Petrarolo, Simone Brogi, Concettina La Motta, Lara Testai, and Vincenzo Calderone.

Dear Editor-in-Chief Professor Martin Brandl, Dear Associate Editor Prof. Cosimo Altomare,

Please find here enclosed the electronic version of the revised manuscript quoted PHASCI-D-21-00589. We have taken into consideration all the indications provided by the reviewers to improve the quality of the manuscript. Moreover, a tracked version of the manuscript has been submitted to easily evaluate the changes done in the manuscript.

If other revisions will be required, we will provide additional changes.

A point to point response to all comments provided by Referees is given below. Facilitating the evaluation of this article is greatly appreciated.

Simone Brogi, M.Sc., Ph.D.
Assistant Professor
Department of Pharmacy, University of Pisa
Via Bonanno 6, 56126, Pisa, Italy
Tel: +390502219613
E-mail: simone.brogi@unipi.it

Reviewer #1: In this manuscript, the authors selected new compounds capable of interacting with SIRT1. In its current form the manuscript cannot be published, as the in silico results section is very bad. Further revisions are needed.

Authors: We thank the referee for his/her careful reading. In order to improve the quality of the manuscript, we have taken into consideration all the comments/suggestions in the revised version of the manuscript.

1. In the Abstract, the authors must briefly report the methodologies used

2. In the abstract, the authors should briefly describe the main results obtained in each methodology. Finally, the authors must inform how these results advance the frontier of knowledge on the topic investigated.

Authors: The abstract has been revised accordingly, introducing methodologies for the screening and highlighting the results obtained from each step of the screening.

3. The introduction must contain a maximum of two pages of text, three pages with the figure included. Authors should be more concise in communicating information.

Authors: The introduction has been shortened as maximum as possible, considering that our writing reported the description of the target, the usefulness to target SIRT1 in several diseases, identified compounds able to modulate this enzyme and the purpose of the work. Considering that the figure is one page we reduced the text to two pages and half.

4. This section is unnecessary "4.1. Computational details". This section has no important information.

Authors: We remove this section accordingly.

5. There is no need to include "DOI: 10.2210 / pdb5BTR / pdb". The reference information [46] is sufficient.

Authors: According to the referee comment, we remove the doi related to the crystal structure used in this study.

6. The protocol used must be reported in the manuscript - "and imported into Maestro suite 2018 and prepared by means of protein preparation wizard protocol for obtaining a suitable starting structure for further computational experiments".

Authors: According to the referee comment, we reported details about the protein preparation wizard protocol. These details have been enclosed in section 4.1.1. Database and protein preparation. Now the part related to the protein preparation is as reported below:

“The three-dimensional structure of the human SIRT1 enzyme was obtained from the Protein Data Bank (PDB ID 5BTR [46]; crystal structure of SIRT1 in complex with resveratrol and an AMC-containing peptide) and imported into Maestro suite 2018 and prepared by means of protein preparation wizard protocol for obtaining a suitable starting structure for further computational experiments [13, 64]. Using this protocol, we performed a series of computational steps to: (1) add hydrogens, (2) optimize the orientation of hydroxyl groups, Asn, and Gln, and the protonation state of His, and (3) perform a constrained minimization refinement using the *impref* utility. In particular, at first, the protein was preprocessed by adding all hydrogen atoms to structure, assigning bond orders, creating disulfide bonds and filling missing side chains and loops. To optimize the hydrogen bond network, His tautomers and ionization states were predicted, 180° rotations of the terminal angle of Asn, Gln, and His residues were assigned, and hydrogen atoms of hydroxyl and thiol groups were sampled. Finally, a restrained minimization was performed using the Impact Refinement (*impref*) module, employing OPLS3 force field to optimize the geometry and minimize the energy of the protein. The minimization was terminated when the energy converged, or the RMSD reached a maximum cutoff of 0.30 Å.

7. Is this library published in any scientific journal? "In this study, we used an in-house library of synthetic molecules designed by taking inspiration from natural compounds."

Authors: We thank the referee for this comment, as she/he gave us a way to improve the clarity of the manuscript. The in-house library used in the study included both pyrido[1,2-a]pyrimidine derivatives, developed as bioisosters of flavonoids, and imidazo[1,2-a]pyridine derivatives, designed as constrained analogs of resveratrol. While the former have already been published in a scientific journal, the latter are original compounds described here for the first time. A proper reference has been inserted in the text (see reference 59 of the manuscript) to make this aspect clearer to the readers.

8. This information should be included only in the methodology "(Glide release 2018, Schrödinger LLC, New York, 2018)," "and (Prime release 2018, Schrödinger LLC, New York, 2018)"

Authors: According to the referee comment the information about the software are now included only in the Experimental section.

9. In all the text below, the authors only describe the methodology used and / or what the method used is for. All the text below is in the results and discussions section In the results and discussions section, the authors must report and discuss their results, however I did not observe this in the manuscript. All of the text below is describing or explaining what the method used is for. That is, this text should not be included in the results and discussions section. In manuscript "The first step of our integrated screening platform is represented by a computational protocol to perform virtual screening of a selected library in order to rapidly identify potential SIRT1 activators. To this end, we combined molecular docking-based approach with the estimation of relative ligand binding energy, using the crystal structure of SIRT1 enzyme in complex with resveratrol as previously described by us [52]. In this study, we used an in-house library of synthetic molecules designed by taking inspiration from natural compounds. Actually, it includes both pyrido[1,2-a]pyrimidine derivatives, developed as bioisosters of flavonoids, and imidazo[1,2-a]pyridine compounds, designed as rigidified and constrained analogues of the natural resveratrol. On the basis of their chemical structures, we assumed that these compounds could share a similar mechanism of SIRT1 activation described for the natural derivatives.

Briefly, as reported in Figure 2, resveratrol activates SIRT1 by targeting a specific region of the enzyme located in its N-terminal domain (NTD). Specifically, resveratrol binds NTD interacting with three distinct binding sites (highlighted as #site1, #site2, and #site3 in Figure 2A), as determined by experimental studies [46]. Moreover, the experimentally solved complex SIRT1/resveratrol was acquired with a specific peptide system (7-amino-4-methylcoumarin AMC-containing peptide), mimicking the p53-interacting residues. This peptide is positioned between NTD and catalytic domain (CD) interfaces (Figure 2A). The identified binding sites diversely contribute in activating SIRT1 enzyme. In fact, mutagenesis studies indicated that the interactions with #site1 and #site2 were found necessary for activating SIRT1, whereas #site3 is demarcated as "accessory site," displaying a lesser impact regarding enzyme activation [46]. Accordingly, two resveratrol molecules facilitate the interaction among the AMC-peptide and the SIRT1-NTD and are extremely relevant for promoting a strong binding between the peptide and SIRT1 stimulating the enzyme activity. Starting from this mechanism of action, we developed a docking protocol able to evaluate the affinity of a molecule into the three distinct binding sites of SIRT1. Accordingly, we submitted the selected library to this protocol, evaluating the affinity of the contained molecules for these binding sites. In order to identify the most promising molecules we retained only the ones showing a favorable affinity for each site comparable or better than that found for resveratrol (Table 1). The affinity for the mentioned binding sites for each molecule was evaluated considering the docking score obtained by Glide software (Glide release 2018, Schrödinger LLC, New York, 2018),

calculated by applying extra precision (XP) as scoring function coupled with a rescoring step employing standard precision (SP) method, combined with the relative ligand binding energy (ΔGbind), calculated by using Prime software employing MM/GBSA technique (Prime release 2018, Schrödinger LLC, New York, 2018).

The second step of our computational protocol consisted of evaluating the drug-like profile of compounds with favorable affinity values as found bye molecular docking calculation. For this purpose, we submitted the retrieved compounds to QikProp software (QikProp release 2018, Schrödinger LLC, New York, 2018) and FAFDrugs4 web-server. From this assessment, we selected only molecules having a drug-like profile more favorable than the one displayed by resveratrol. In fact, as reported in Table 1, the identified compounds showed satisfactory LogP and solubility (LogS) along with a good capacity to cross membranes as suggested from the values of the prediction regarding the models of permeability, taking into account Caco-2 and MDCK cells. In fact, QPPCaco (model for the gut-blood barrier) predicts apparent Caco-2 cell permeability in nm/sec, while QPPMDCK (model for the for the blood brain barrier) predicts apparent MDCK cell permeability in nm/sec. Remarkably, QikProp predictions are for non-active transport. In addition, the potential SIRT1 activators were predicted to be devoid of cardiotoxicity. The assessment of oral absorption showed a favorable predicted profile for the identified compounds with respect to resveratrol. Furthermore, QikProp calculation highlighted the scarce pharmacokinetic profile for resveratrol as largely reported in literature. In addition, the output of FAFDrugs4 [59] showed that the screened compounds are not pan-assay interference compounds (PAINS), although the output highlighted a low risk warning for compounds containing phenol and catechol moiety."

10. The entire section of results and discussions on the in silico protocol must be rewritten.

Authors: In order to fulfill the referee requests we moved the information highlighted by the referee in the Materials and Methods, keeping only the discussion (shortened) on the development of the protocol, and the output of the results reported in Table 1, along with the discussion of the binding mode of the representative compound enclosed in Figure 2. Instead we preferred to maintain the brief discussion about the mechanism of action of resveratrol since is indicative for evaluating the performance of the screened compounds and for understanding the development of the in silico protocol. However, as requested, the section is now cleaned from the details that can be enclosed in the Materials and Methods section and the discussion on results was added. So, the section has been rewritten accordingly. For your consideration a tracked version of the manuscript was uploaded for easily evaluate the changes.

11. The docking protocol needs to be validated. For this, the authors must perform the redocking and the RMSD between the redocked ligand and the crystallized ligand must be less than 2 angstroms. The following works carried out this protocol and can serve to enrich the references in this manuscript: https://doi.org/10.1080/07391102.2020.1796791 ; https://doi.org/10.1080/07391102.2020.1761878 ; https://doi.org/10.3390/PH13090209 ; https://doi.org/10.3390/MOLECULES25184183 ; https://doi.org/10.1080/07391102.2020.1839562

Authors: We thank the referee for this observation. Accordingly, we added full details about our docking validation protocol. Moreover, we also added a picture (Figure S1), highlighting the output of the validation protocol. In the experimental section, we modified the text providing the data about this step also introducing suggested references (in the main text [65-69]).

"In particular, the calculation of the root-mean-square deviation (RMSD), performed using the tool available in Maestro suite, showed a lower value between the crystallized structure and the docked pose of resveratrol for each selected binding site (#site1, RMSD 0.148 Å; #site2, RMSD 0.143 Å; #site3, RMSD 0.151 Å). This procedure is a well-established technique for validating the docking protocol employed in virtual screening campaigns [65-69]."

As argued by the referee for validating the protocol the RMSD should be lower than 2 Å, and in this case our results are in line with this statement since for each selected binding site, the RMSD between the crystallized ligand and redocked ligand is lower than 2 Å.

Reviewer #2: The proposal is to find novel SIRT1 activator molecules using in silico screening, followed by synthesis and in vitro and ex vivo screening of key compounds. This has become a more routine strategy rather than innovative.

Authors: We thank the referee for his/her careful reading. In order to improve the quality of the manuscript, we have taken into consideration all the comments/suggestions in the revised version of the manuscript. As argued by the referee, due to our interest in searching molecules possessing cardioprotective profile targeting different targets, in this work we developed an integrated screening platform for a rapid identification of compounds endowed with cardioprotective profile targeting SIRT1 enzyme. Methods are not innovative, but starting with computational studies integrating medicinal chemistry and pharmacology, we developed an accurate screening method allowing us to select a small number of compounds that significantly activate SIRT1, saving time and money with respect to the high throughput screening method.

A focused screening library was employed:"in-house library of synthetic molecules designed by taking inspiration from natural compounds. Actually, it includes both pyrido[1,2-a]pyrimidine

derivatives, developed as bioisosters of flavonoids, and imidazo[1,2-a]pyridine compounds, designed as rigidified and constrained analogues of the natural resveratrol." How large was this library? How can the hit rate be evaluated objectively?

Authors: We thank the referee for the comment, as she/he gave us a way to improve the clarity of the manuscript. The in-house library used in the study (54 compounds) included both already described pyrido[1,2-a]pyrimidine derivatives (see reference 59 of the manuscript), and original imidazo[1,2-a]pyridine derivatives, described here for the first time. Representative examples of the two series have been taken into account in the study, achieving a total of 11 compounds.

Regarding the success rate of our protocol, we would like to highlight that the virtual screening procedure reported a success in identifying hit compounds around 40% considering the hit rates. Accordingly, our screening protocol is in line with this value since 5 of 11 compounds behave as SIRT1 activators (hit rate 45%) this discussion was also reported in the main text.

Plausible binding modes for library compounds described, based upon existing crystal structures.

Based on the affinities for the three binding sites, could the 11 compounds be put in rank order?

How does the binding affinity explain the low activity of compounds 1, 5?

It this set of 11 compounds meaningful as regards SAR?

Authors: We thank the referee for this observation. Due to the three binding sites, there is no way to have a clear rank of screened compounds, since some of them showed better docking score for one site or better ΔGbind for the other ones. The purpose of the screening is to identify compounds performing better than the reference molecules in terms of docking score ΔGbind and ADME profile.

Regarding the second point, there is no clear indication about the low activity of compounds 1 and 5 based on the binding affinity. Only for compound 1 we observed that the computational scores are lower than the other compounds and we expected that this compound could not a strong activator as found in the in vitro tests. However, as mentioned in the previous comment, our screening protocol showed a hit rate of 45%.

Finally, due to the heterogeneous structures identified, the retrieved compounds are not meaningful regarding SAR studies. In particular, with these compounds is not possible to cover a sufficient chemical space for providing an exhaustive SAR analysis. This step can be performed only considering the identified hit (compound **8**) by synthesizing a significant number of analogs for covering sufficient chemical space. This step was under consideration in our labs in an attempt to optimize compound **8**.

Previous attempts to develop SIRT1 activators was noted.

"these potential drug candidates showed in general poor and variable pharmacokinetics upon oral administration.""Compounds 2 (GP36), 3 (GP35), 7 (GP46) and 10 (GP27d) were discontinued from the test due to the inconsistency of the results" Variable pharmacokinetics remains an unsolved issue.

Authors: We thank the referee for this observation. The pharmacokinetics problems related to the developed compounds in the introduction were not refereed to the selected compounds in this study. In fact, all selected compounds, according to the in silico prediction, showed good solubility with no relevant issues about their application. Unfortunately, compounds 2 (GP36), 3 (GP35), 7 (GP46) and 10 (GP27d) have been discontinued from the in vitro test because they are colored. We tried testing them, nevertheless interference with the probe of the assay kit caused the inconsistency of the results. This aspect was unpredictable and we were forced to deprioritize the above-mentioned compounds from further studies.

"the screened compounds are not pan-assay interference compounds (PAINS), although the output highlighted a low risk warning for compounds containing phenol and catechol moiety"

Metabolism and clearance of phenols and related compounds are well known issues but are not addressed here in compound design. QuikProp data does not appear to assess these issues.

The compounds are not expected to be PAINS but there is no further information for off-target activity.

Authors: As argued by the referee, QikProp cannot perform the step regarding the assessment of Pan Assay Interference Compounds (PAINS). In fact, for this purpose, we used FAFDrugs4 web-server. This step is highlighted in the Results and Discussion section as well as in the Experimental section (4.1.2. Evaluation of drug-like profile). Regarding possible off-target activity, we reported the calculation of QPlogHERG (Table 1) available in QikProp, that predicted IC_{50} values for blockage of HERG K^+ channels. Based on the above-mentioned calculation, the selected compounds don't possess hERG liability. Moreover, the purpose of the work is to provide a validation of our integrated screening protocol for identifying SIRT1 activators, at this stage metabolism and clearance of phenols were not taken into consideration since compounds were not designed but they belong to our in-house library containing synthetic molecules inspired by nature, including both bioisosters of natural flavonoids and rigidified and constrained analogues of resveratrol. The mentioned point can be taken into consideration in the ligand-optimization step that is currently ongoing in our lab.

Abstract

Drugs targeting epigenetic mechanisms are attracting the attention of scientists since it was observed that the modulation of this post-translational apparatus, could help to identify innovative therapeutic strategies. Among the epigenetic druggable targets, the positive modulation of SIRT1 has also been related to significant cardioprotective effects. Unfortunately, actual SIRT1 activators (natural products and synthetic molecules) suffer from several drawbacks, particularly poor pharmacokinetic profiles. Accordingly, in this article we present the development of an integrated screening platform aimed at identifying novel SIRT1 activators with favorable drug-like features as cardioprotective agents. Encompassing several competencies (*in silico*, medicinal chemistry, and pharmacology), we describe a multidisciplinary approach for rapidly identifying SIRT1 activators and their preliminary pharmacological characterization. In the first step, we virtually screened an in-house chemical library comprising synthetic molecules inspired by nature, against SIRT1 enzyme. To this end, we combined molecular docking-based approach with the estimation of relative ligand binding energy, using the crystal structure of SIRT1 enzyme in complex with resveratrol. Eleven computational hits were identified synthesized and tested against the isolated enzyme for validating the *in silico* strategy. Among the tested molecules, five of them behave as SIRT1 enzyme activators. Due to the superior response in activating the enzyme and its favorable calculated physico-chemical properties, compound **8** was further characterized in *ex vivo* studies on isolated and perfused rat hearts submitted to ischemia/reperfusion (I/R) period. The pharmacological profile of compound **8**, suggests that this molecule represents a prototypic SIRT1 activator with satisfactory drug-like profile, paving the way for developing novel epigenetic cardioprotective agents.

Reviewer #1: In this manuscript, the authors selected new compounds capable of interacting with SIRT1. In its current form the manuscript cannot be published, as the in silico results section is very bad. Further revisions are needed.

Authors: We thank the referee for his/her careful reading. In order to improve the quality of the manuscript, we have taken into consideration all the comments/suggestions in the revised version of the manuscript.

1. In the Abstract, the authors must briefly report the methodologies used

2. In the abstract, the authors should briefly describe the main results obtained in each methodology. Finally, the authors must inform how these results advance the frontier of knowledge on the topic investigated.

Authors: The abstract has been revised accordingly, introducing methodologies for the screening and highlighting the results obtained from each step of the screening.

3. The introduction must contain a maximum of two pages of text, three pages with the figure included. Authors should be more concise in communicating information.

Authors: The introduction has been shortened as maximum as possible, considering that our writing reported the description of the target, the usefulness to target SIRT1 in several diseases, identified compounds able to modulate this enzyme and the purpose of the work. Considering that the figure is one page we reduced the text to two pages and half.

4. This section is unnecessary "4.1. Computational details". This section has no important information.

Authors: We remove this section accordingly.

5. There is no need to include "DOI: 10.2210 / pdb5BTR / pdb". The reference information [46] is sufficient.

Authors: According to the referee comment, we remove the doi related to the crystal structure used in this study.

6. The protocol used must be reported in the manuscript - "and imported into Maestro suite 2018 and prepared by means of protein preparation wizard protocol for obtaining a suitable starting structure for further computational experiments".

Authors: According to the referee comment, we reported details about the protein preparation wizard protocol. These details have been enclosed in section 4.1.1. Database and protein preparation. Now the part related to the protein preparation is as reported below:

“The three-dimensional structure of the human SIRT1 enzyme was obtained from the Protein Data Bank (PDB ID 5BTR [46]; crystal structure of SIRT1 in complex with resveratrol and an AMC-containing peptide) and imported into Maestro suite 2018 and prepared by means of protein preparation wizard protocol for obtaining a suitable starting structure for further computational experiments [13, 64]. Using this protocol, we performed a series of computational steps to: (1) add hydrogens, (2) optimize the orientation of hydroxyl groups, Asn, and Gln, and the protonation state of His, and (3) perform a constrained minimization refinement using the *impref* utility. In particular, at first, the protein was preprocessed by adding all hydrogen atoms to structure, assigning bond orders, creating disulfide bonds and filling missing side chains and loops. To optimize the hydrogen bond network, His tautomers and ionization states were predicted, 180° rotations of the terminal angle of Asn, Gln, and His residues were assigned, and hydrogen atoms of hydroxyl and thiol groups were sampled. Finally, a restrained minimization was performed using the Impact Refinement (*impref*) module, employing OPLS3 force field to optimize the geometry and minimize the energy of the protein. The minimization was terminated when the energy converged, or the RMSD reached a maximum cutoff of 0.30 Å.

7. Is this library published in any scientific journal? "In this study, we used an in-house library of synthetic molecules designed by taking inspiration from natural compounds."

Authors: We thank the referee for this comment, as she/he gave us a way to improve the clarity of the manuscript. The in-house library used in the study included both pyrido[1,2-a]pyrimidine derivatives, developed as bioisosters of flavonoids, and imidazo[1,2-a]pyridine derivatives, designed as constrained analogs of resveratrol. While the former have already been published in a scientific journal, the latter are original compounds described here for the first time. A proper reference has been inserted in the text (see reference 59 of the manuscript) to make this aspect clearer to the readers.

8. This information should be included only in the methodology "(Glide release 2018, Schrödinger LLC, New York, 2018)," "and (Prime release 2018, Schrödinger LLC, New York, 2018)"

Authors: According to the referee comment the information about the software are now included only in the Experimental section.

9. In all the text below, the authors only describe the methodology used and / or what the method used is for. All the text below is in the results and discussions section In the results and discussions section, the authors must report and discuss their results, however I did not observe this in the manuscript. All of the text below is describing or explaining what the method used is for. That is, this text should not be included in the results and discussions section. In manuscript "The first step of our integrated screening platform is represented by a computational protocol to perform virtual screening of a selected library in order to rapidly identify potential SIRT1 activators. To this end, we combined molecular docking-based approach with the estimation of relative ligand binding energy, using the crystal structure of SIRT1 enzyme in complex with resveratrol as previously described by us [52]. In this study, we used an in-house library of synthetic molecules designed by taking inspiration from natural compounds. Actually, it includes both pyrido[1,2-a]pyrimidine
derivatives, developed as bioisosters of flavonoids, and imidazo[1,2-a]pyridine compounds, designed as rigidified and constrained analogues of the natural resveratrol. On the basis of their chemical structures, we assumed that these compounds could share a similar mechanism of SIRT1 activation described for the natural derivatives.

Briefly, as reported in Figure 2, resveratrol activates SIRT1 by targeting a specific region of the enzyme located in its N-terminal domain (NTD). Specifically, resveratrol binds NTD interacting with three distinct binding sites (highlighted as #site1, #site2, and #site3 in Figure 2A), as determined by experimental studies [46]. Moreover, the experimentally solved complex SIRT1/resveratrol was acquired with a specific peptide system (7-amino-4-methylcoumarin AMC-containing peptide), mimicking the p53-interacting residues. This peptide is positioned between NTD and catalytic domain (CD) interfaces (Figure 2A). The identified binding sites diversely contribute in activating SIRT1 enzyme. In fact, mutagenesis studies indicated that the interactions with #site1 and #site2 were found necessary for activating SIRT1, whereas #site3 is demarcated as "accessory site," displaying a lesser impact regarding enzyme activation [46]. Accordingly, two resveratrol molecules facilitate the interaction among the AMC-peptide and the SIRT1-NTD and are extremely relevant for promoting a strong binding between the peptide and SIRT1 stimulating the enzyme activity. Starting from this mechanism of action, we developed a docking protocol able to evaluate the affinity of a molecule into the three distinct binding sites of SIRT1. Accordingly, we submitted the selected library to this protocol, evaluating the affinity of the contained molecules for these binding sites. In order to identify the most promising molecules we retained only the ones showing a favorable affinity for each site comparable or better than that found for resveratrol (Table 1). The affinity for the mentioned binding sites for each molecule was evaluated considering the docking score obtained by Glide software (Glide release 2018, Schrödinger LLC, New York, 2018), calculated by applying extra precision (XP)

as scoring function coupled with a rescoring step employing standard precision (SP) method, combined with the relative ligand binding energy (ΔGbind), calculated by using Prime software employing MM/GBSA technique (Prime release 2018, Schrödinger LLC, New York, 2018).

The second step of our computational protocol consisted of evaluating the drug-like profile of compounds with favorable affinity values as found bye molecular docking calculation. For this purpose, we submitted the retrieved compounds to QikProp software (QikProp release 2018, Schrödinger LLC, New York, 2018) and FAFDrugs4 web-server. From this assessment, we selected only molecules having a drug-like profile more favorable than the one displayed by resveratrol. In fact, as reported in Table 1, the identified compounds showed satisfactory LogP and solubility (LogS) along with a good capacity to cross membranes as suggested from the values of the prediction regarding the models of permeability, taking into account Caco-2 and MDCK cells. In fact, QPPCaco (model for the gut-blood barrier) predicts apparent Caco-2 cell permeability in nm/sec, while QPPMDCK (model for the for the blood brain barrier) predicts apparent MDCK cell permeability in nm/sec. Remarkably, QikProp predictions are for non-active transport. In addition, the potential SIRT1 activators were predicted to be devoid of cardiotoxicity. The assessment of oral absorption showed a favorable predicted profile for the identified compounds with respect to resveratrol. Furthermore, QikProp calculation highlighted the scarce pharmacokinetic profile for resveratrol as largely reported in literature. In addition, the output of FAFDrugs4 [59] showed that the screened compounds are not pan-assay interference compounds (PAINS), although the output highlighted a low risk warning for compounds containing phenol and catechol moiety."

10. The entire section of results and discussions on the in silico protocol must be rewritten.

Authors: In order to fulfill the referee requests we moved the information highlighted by the referee in the Materials and Methods, keeping only the discussion (shortened) on the development of the protocol, and the output of the results reported in Table 1, along with the discussion of the binding mode of the representative compound enclosed in Figure 2. Instead we preferred to maintain the brief discussion about the mechanism of action of resveratrol since is indicative for evaluating the performance of the screened compounds and for understanding the development of the in silico protocol. However, as requested, the section is now cleaned from the details that can be enclosed in the Materials and Methods section and the discussion on results was added. So, the section has been rewritten accordingly. For your consideration a tracked version of the manuscript was uploaded for easily evaluate the changes.

11. The docking protocol needs to be validated. For this, the authors must perform the redocking and the RMSD between the redocked ligand and the crystallized ligand must be less than 2 angstroms.

The following works carried out this protocol and can serve to enrich the references in this manuscript: https://doi.org/10.1080/07391102.2020.1796791 ; https://doi.org/10.1080/07391102.2020.1761878 ; https://doi.org/10.3390/PH13090209 ; https://doi.org/10.3390/MOLECULES25184183 ; https://doi.org/10.1080/07391102.2020.1839562

Authors: We thank the referee for this observation. Accordingly, we added full details about our docking validation protocol. Moreover, we also added a picture (Figure S1), highlighting the output of the validation protocol. In the experimental section, we modified the text providing the data about this step also introducing suggested references (in the main text [65-69]).

"In particular, the calculation of the root-mean-square deviation (RMSD), performed using the tool available in Maestro suite, showed a lower value between the crystallized structure and the docked pose of resveratrol for each selected binding site (#site1, RMSD 0.148 Å; #site2, RMSD 0.143 Å; #site3, RMSD 0.151 Å). This procedure is a well-established technique for validating the docking protocol employed in virtual screening campaigns [65-69]."

As argued by the referee for validating the protocol the RMSD should be lower than 2 Å, and in this case our results are in line with this statement since for each selected binding site, the RMSD between the crystallized ligand and redocked ligand is lower than 2 Å.

Reviewer #2: The proposal is to find novel SIRT1 activator molecules using in silico screening, followed by synthesis and in vitro and ex vivo screening of key compounds. This has become a more routine strategy rather than innovative.

Authors: We thank the referee for his/her careful reading. In order to improve the quality of the manuscript, we have taken into consideration all the comments/suggestions in the revised version of the manuscript. As argued by the referee, due to our interest in searching molecules possessing cardioprotective profile targeting different targets, in this work we developed an integrated screening platform for a rapid identification of compounds endowed with cardioprotective profile targeting SIRT1 enzyme. Methods are not innovative, but starting with computational studies integrating medicinal chemistry and pharmacology, we developed an accurate screening method allowing us to select a small number of compounds that significantly activate SIRT1, saving time and money with respect to the high throughput screening method.

A focused screening library was employed:"in-house library of synthetic molecules designed by taking inspiration from natural compounds. Actually, it includes both pyrido[1,2-a]pyrimidine

derivatives, developed as bioisosters of flavonoids, and imidazo[1,2-a]pyridine compounds, designed as rigidified and constrained analogues of the natural resveratrol." How large was this library? How can the hit rate be evaluated objectively?

Authors: We thank the referee for the comment, as she/he gave us a way to improve the clarity of the manuscript. The in-house library used in the study (54 compounds) included both already described pyrido[1,2-a]pyrimidine derivatives (see reference 59 of the manuscript), and original imidazo[1,2-a]pyridine derivatives, described here for the first time. Representative examples of the two series have been taken into account in the study, achieving a total of 11 compounds.

Regarding the success rate of our protocol, we would like to highlight that the virtual screening procedure reported a success in identifying hit compounds around 40% considering the hit rates. Accordingly, our screening protocol is in line with this value since 5 of 11 compounds behave as SIRT1 activators (hit rate 45%) this discussion was also reported in the main text.

Plausible binding modes for library compounds described, based upon existing crystal structures.

Based on the affinities for the three binding sites, could the 11 compounds be put in rank order?

How does the binding affinity explain the low activity of compounds 1, 5?

It this set of 11 compounds meaningful as regards SAR?

Authors: We thank the referee for this observation. Due to the three binding sites, there is no way to have a clear rank of screened compounds, since some of them showed better docking score for one site or better ΔGbind for the other ones. The purpose of the screening is to identify compounds performing better than the reference molecules in terms of docking score ΔGbind and ADME profile.

Regarding the second point, there is no clear indication about the low activity of compounds 1 and 5 based on the binding affinity. Only for compound 1 we observed that the computational scores are lower than the other compounds and we expected that this compound could not a strong activator as found in the in vitro tests. However, as mentioned in the previous comment, our screening protocol showed a hit rate of 45%.

Finally, due to the heterogeneous structures identified, the retrieved compounds are not meaningful regarding SAR studies. In particular, with these compounds is not possible to cover a sufficient chemical space for providing an exhaustive SAR analysis. This step can be performed only considering the identified hit (compound **8**) by synthesizing a significant number of analogs for covering sufficient chemical space. This step was under consideration in our labs in an attempt to optimize compound **8**.

Previous attempts to develop SIRT1 activators was noted.

"these potential drug candidates showed in general poor and variable pharmacokinetics upon oral administration.""Compounds 2 (GP36), 3 (GP35), 7 (GP46) and 10 (GP27d) were discontinued from the test due to the inconsistency of the results" Variable pharmacokinetics remains an unsolved issue.
Authors: We thank the referee for this observation. The pharmacokinetics problems related to the developed compounds in the introduction were not refereed to the selected compounds in this study. In fact, all selected compounds, according to the in silico prediction, showed good solubility with no relevant issues about their application. Unfortunately, compounds 2 (GP36), 3 (GP35), 7 (GP46) and 10 (GP27d) have been discontinued from the in vitro test because they are colored. We tried testing them, nevertheless interference with the probe of the assay kit caused the inconsistency of the results. This aspect was unpredictable and we were forced to deprioritize the above-mentioned compounds from further studies.

"the screened compounds are not pan-assay interference compounds (PAINS), although the output highlighted a low risk warning for compounds containing phenol and catechol moiety"
Metabolism and clearance of phenols and related compounds are well known issues but are not addressed here in compound design. QuikProp data does not appear to assess these issues.
The compounds are not expected to be PAINS but there is no further information for off-target activity.
Authors: As argued by the referee, QikProp cannot perform the step regarding the assessment of Pan Assay Interference Compounds (PAINS). In fact, for this purpose, we used FAFDrugs4 web-server. This step is highlighted in the Results and Discussion section as well as in the Experimental section (4.1.2. Evaluation of drug-like profile). Regarding possible off-target activity, we reported the calculation of QPlogHERG (Table 1) available in QikProp, that predicted IC_{50} values for blockage of HERG K^+ channels. Based on the above-mentioned calculation, the selected compounds don't possess hERG liability. Moreover, the purpose of the work is to provide a validation of our integrated screening protocol for identifying SIRT1 activators, at this stage metabolism and clearance of phenols were not taken into consideration since compounds were not designed but they belong to our in-house library containing synthetic molecules inspired by nature, including both bioisosters of natural flavonoids and rigidified and constrained analogues of resveratrol. The mentioned point can be taken into consideration in the ligand-optimization step that is currently ongoing in our lab.

Highlights

- An integrated screening platform was developed for identifying SIRT1 activators
- A virtual screening of a focused in-house chemical library against SIRT1 was performed
- The retrieved computational hits were synthesized and tested against the isolated enzyme
- The most promising compound was evaluated in an *ex vivo* model of isolated rat hearts submitted to I/R period
- Compound **8** showed a significant cardioprotective profile, along with favourable drug-like features

Graphical Abstract

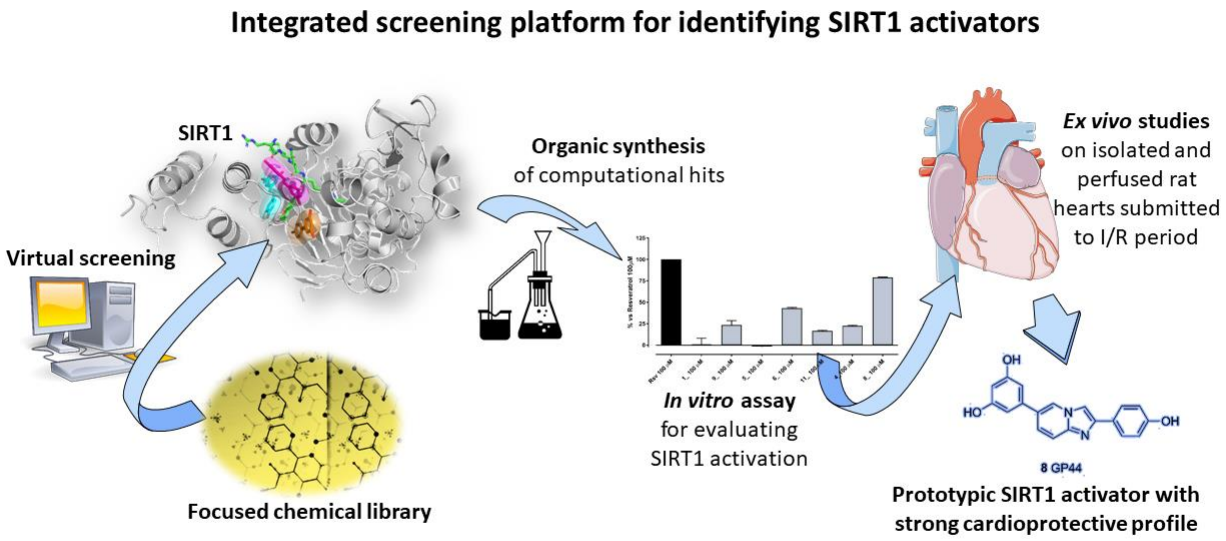

Identification of Novel SIRT1 Activators Endowed with Cardioprotective Profile

Lorenzo Flori[a,1], Giovanni Petrarolo[a,1], Simone Brogi[a,*], Concettina La Motta[a,**], Lara Testai[a,***], Vincenzo Calderone[a]

[a]*Department of Pharmacy, University of Pisa, Via Bonanno, 6, I-56126 Pisa, Italy*

[1]These authors contributed equally to this work

Corresponding Authors:

*Simone Brogi, email: simone.brogi@unipi.it

**Concettina La Motta (medicinal chemistry), email: concettina.lamotta@unipi.it

***Lara Testai (pharmacology), email: lara.testai@unipi.it

Abstract

Drugs targeting epigenetic mechanisms are attracting the attention of scientists since it was observed that the modulation of this post-translational apparatus, could help to identify innovative therapeutic strategies. Among the epigenetic druggable targets, the positive modulation of SIRT1 has also been related to significant cardioprotective effects. Unfortunately, actual SIRT1 activators (natural products and synthetic molecules) suffer from several drawbacks, particularly poor pharmacokinetic profiles. Accordingly, in this article we present the development of an integrated screening platform aimed at identifying novel SIRT1 activators with favorable drug-like features as cardioprotective agents. Encompassing several competencies (*in silico*, medicinal chemistry, and pharmacology), we describe a multidisciplinary approach for rapidly identifying SIRT1 activators and their preliminary pharmacological characterization. In the first step, we virtually screened an in-house chemical library comprising synthetic molecules inspired by nature, against SIRT1 enzyme. To this end, we combined molecular docking-based approach with the estimation of relative ligand binding energy, using the crystal structure of SIRT1 enzyme in complex with resveratrol. Eleven computational hits were identified synthesized and tested against the isolated enzyme for validating the *in silico* strategy. Among the tested molecules, five of them behave as SIRT1 enzyme activators. Due to the superior response in activating the enzyme and its favorable calculated physico-chemical properties, compound **8** was further characterized in *ex vivo* studies on isolated and perfused rat hearts submitted to ischemia/reperfusion (I/R) period. The pharmacological profile of compound **8**, suggests that this molecule represents a prototypic SIRT1 activator with satisfactory drug-like profile, paving the way for developing novel epigenetic cardioprotective agents.

Keywords: SIRT1 activators, epigenetics, cardioprotection, computer-aided drug discovery, organic synthesis, pyrido[1,2-*a*]pyrimidin-4-ones, imidazo[1,2-*a*]pyridines.

1. Introduction

Nicotinamide adenine dinucleotide (NAD^+)-dependent deacetylase and/or ADP-ribosylase enzymes, namely, sirtuins (SIRTs, silent information regulator genes) belong to the protein superfamily of histone deacetylase (HDAC) [1, 2]. This latter modulates the epigenetic cellular machinery, playing a crucial role in gene regulation, being able to interact with several histone and non-histone substrates [3, 4]. This family is currently divided into four classes and eighteen members. Along with the mentioned class III SIRTs (SIRT1-7) [5], HDACs are classified on the basis of domains organization, functions, cellular localization, and sequence homology to yeast-related proteins (HDAC1-11, class I: HDAC1-3, HDAC8; class II (IIa: HDAC4,5, HDAC7, HDAC9, and IIb: HDAC6, HDAC10); class IV: HDAC11) [6]. Dysregulation of fine-tuning deacetylase cellular activity has been observed in several human diseases, including cancers, cardiovascular diseases, metabolic syndromes, and neurodegenerative disorders [7-10]. Recently, altered expression of HDAC family members has been observed in numerous rare diseases [11, 12]. In this scenario, the modulation of deacetylase activity by inhibitors and activators has been proposed as a valuable approach for developing innovative therapeutics for treating the mentioned diseases [13-16].

Among the human SIRTs, SIRT1 has been the most investigated isoform. This enzyme is implicated in several biological processes [21], being able to deacetylate numerous non-histone targets [22, 23]. According to numerous transcription factors behaving as substrate of SIRT1, this enzyme has emerged as a crucial interplay in many physiological and pathological conditions. In fact, it has been demonstrated that SIRT1 regulation is directly involved in cellular senescence [24], activating DNA repair machinery [25], genome integrity [26], cardiovascular disorders [27, 28], cancer [29], environmental and cellular stresses [30, 31], age-related pathologies [32], renal and metabolic diseases [33, 34], viral infection and transactivation [35], female fertility [36], inflammation [37], and neurodegenerative disorders [38, 39].

Due to the implication of SIRT1 in regulating several pathways linked to human diseases described above, small-molecules able to negatively and positively affect the activity of SIRT1 are emerging as interesting pharmacological tools in many disorders [15]. Accordingly, while SIRT1 inhibitors can represent the starting point for developing effective drugs against cancers and inflammatory diseases [15, 40], SIRT1 activators are pivotal for developing innovative therapeutics against cardiovascular disorders, aging, age-related and neurodegenerative diseases and metabolic syndrome [41-45].

In particular, in the last decade, numerous compounds from natural sources and synthetic molecules have been identified as SIRT1 activators. Among them, one of the most studied is resveratrol (Figure 1). This natural polyphenol has been characterized as SIRT1 activator by directly binding to the enzyme [46]. This binding produces an activation of the enzyme that is relevant in several animal models of disorders (cardiovascular and neurodegenerative) [47, 48]. Along with resveratrol and its metabolite piceatannol [49], other natural compounds such as quercetin, fisetin, vitexin, orientin, naringenin, curcumin, *trans*-(−)-ε-viniferin, ginsenoside Rc and berberine were found to behave as SIRT1 activators (Figure 1) [49-53]. Unfortunately, the low bioavailability and rapid metabolism of natural products can preclude their effective clinical use. Today, new formulations of these compounds, especially made for resveratrol and curcumin, are under investigation to improve their pharmacokinetic profile [54]. Along with natural products, different small-molecules have been identified as SIRT1 activators through computational and medicinal chemistry approaches [55-57]. Among them, small-molecules acting as SIRT1 activators (e.g. SRT1460, SRT2104, SRT2183, and SRT3025, Figure 1) developed by Sirtris Pharmaceuticals (GlaxoSmithKline) advanced into clinical studies, with SRT2104 involved in several clinical trials. Unfortunately, these potential drug candidates showed in general poor and variable pharmacokinetics upon oral administration. Several attempts aimed at reducing pharmacokinetic inconsistency have also been described, for example, by employing different formulations of the compound SRT2104, although without any appreciable results [58]. In view of that, the search for SIRT1 activators with satisfactory drug-like profile is still a challenging task.

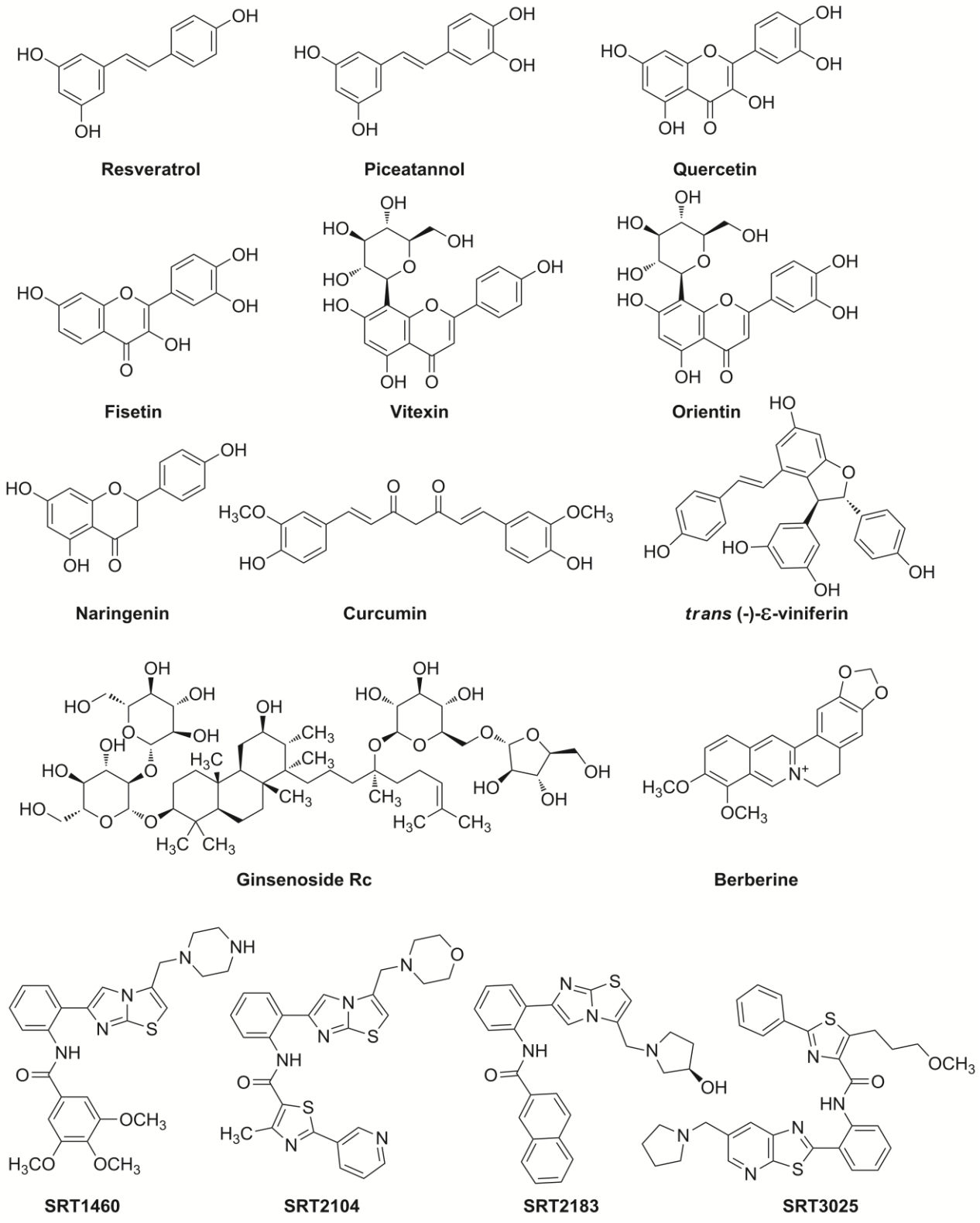

Figure 1. Natural and synthetic compounds acting as SIRT1 activators.

In this framework, pursuing our interest in SIRT1 activation related to cardioprotection, and using a multidisciplinary approach, we succeeded in identifying novel SIRT1 activators as cardioprotective agents by combining *in silico* techniques, organic synthesis, *in vitro* evaluation and *ex vivo* studies.

Starting from a structure-based approach based on molecular docking and relative ligand binding energy, and taking into account the mechanism of action of resveratrol [46], we computationally screened a focused in-house library of synthetic molecules inspired by natural compounds, including both known [59] and original compounds to find compounds sharing a similar mechanism of SIRT1 allosteric activation. The identified *in silico* hits were further screened on the bases of their drug-like profile, to select molecules with potential SIRT1 activator profile endowed with favorable physico-chemical properties. The final hits obtained from this computational protocol were then synthesized in appropriate amounts for further characterization. In fact, to validate the observed *in silico* activities, compounds were investigated *in vitro* for their capability to activate SIRT1 enzyme. Moreover, a compound showing the most potent SIRT1-activating profile, namely, 5-(2-(4-hydroxyphenyl)imidazo[1,2-*a*]pyridin-6-yl)benzene-1,3-diol (**8**, GP44; Table 1), was assessed for its potential as cardioprotective agent on isolated and perfused rat hearts submitted to ischemia/reperfusion (I/R) period. Following this screening platform, it has been possible to rapidly identify SIRT1 activators with significant cardioprotective profile.

2. Results and discussion

2.1. In silico screening of potential SIRT1 activators

In the first step of our integrated screening platform, we performed a virtual screening of a chemical library to rapidly identify potential SIRT1 activators. To this end, we combined molecular docking-based approach with the estimation of relative ligand binding energy, using the crystal structure of SIRT1 enzyme in complex with resveratrol as previously described by us [52]. In this study, we used an in-house library of synthetic molecules designed by taking inspiration from natural compounds, including constrained analogs of resveratrol. On the basis of their chemical structures, we hypothesized that these compounds might share the same mechanism of SIRT1 activation described for the natural derivatives.

Briefly, resveratrol activates SIRT1 by targeting a specific region of the enzyme located in its N-terminal domain (NTD) (Figure 2A). Specifically, resveratrol binds NTD interacting with three distinct binding sites (highlighted as #site1, #site2, and #site3 in Figure 2A), as determined by experimental studies [46]. Moreover, the experimentally solved complex SIRT1/resveratrol was acquired with a specific peptide system (7-amino-4-methylcoumarin AMC-containing peptide), mimicking the p53-interacting residues. This peptide is positioned between NTD and catalytic domain (CD) interfaces (Figure 2A). The identified binding sites diversely contribute in activating SIRT1 enzyme. In fact, mutagenesis studies indicated that the interactions with #site1 and #site2 were found necessary for activating SIRT1, whereas #site3 is demarcated as "accessory site," displaying a lesser impact regarding enzyme activation [46]. Accordingly, two resveratrol molecules facilitate the interaction among the AMC-peptide and the SIRT1-NTD and are extremely relevant for promoting a strong binding between the peptide and SIRT1 stimulating the enzyme activity.

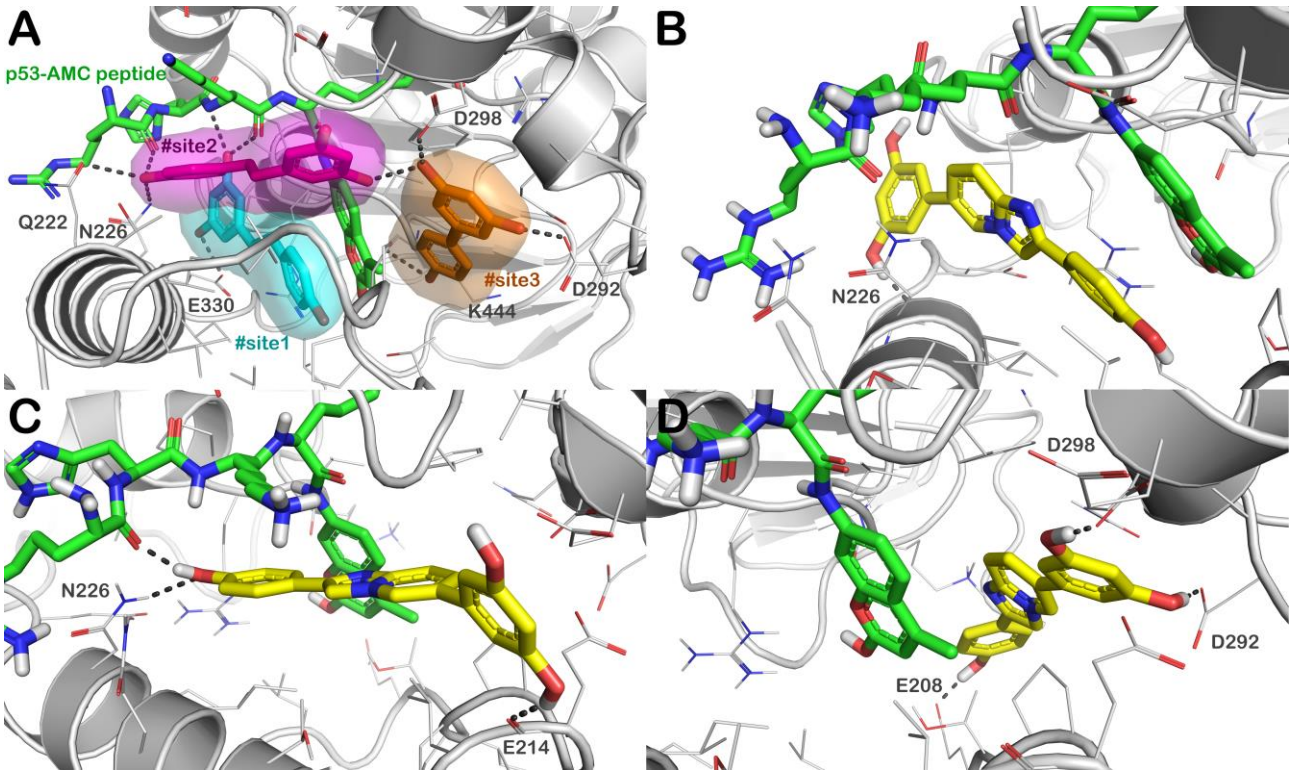

Figure 2. (A) Cristal structure of SIRT1 (grey cartoon representation) in complex with resveratrol (sticks representation) (PDB ID 5BTR); the different binding sites of resveratrol, namely, #site1, #site2 and #site3 are represented in cyan, magenta, and orange, respectively; **(B)** binding mode of

compound **8** (GP44, yellow sticks) into SIRT1 with particular focus on #site1, #site2 **(C)** and #site3 **(D)**. The p53-AMC-peptide is reported as green sticks. Residues in the binding sites are illustrated by lines while hydrogen bonds are indicated as grey dotted lines. Pictures were produced employing PyMOL software (The PyMOL Molecular Graphics System, v1.8; Schrödinger, LLC, New York, 2015).

Starting from this mechanism of action, we developed a docking protocol able to evaluate the affinity of a molecule into the three distinct binding sites of SIRT1. Accordingly, we used this methodology to evaluate the affinity of the molecules contained in the collection for these binding sites. To identify the most promising molecules we retained only the ones showing a favorable affinity for each site comparable or better than that found for resveratrol (Table 1). The affinity for the mentioned binding sites for each molecule was evaluated considering the docking score combined with the relative ligand binding energy (ΔG_{bind}) (full details of the computational protocol are reported in Materials and Methods section). The calculation allowed us to identify compounds showing a docking score for the three selected binding sites comparable or better to that found for resveratrol. In particular, regarding #site1 we found a docking score ranging from -6.32 kcal/mol for compound **1** (GP14) to -8.62 kcal/mol for compound **6** (GP37), while the ΔG_{bind} ranging from -81.6 kcal/mol for compound **1** to -107.4 kcal/mol for compound **10** (GP27d). Considering the #site2 we found a docking score ranging from -6.18 kcal/mol for compound **3** (GP35) to -7.36 kcal/mol for compound **5** (GP32), while the ΔG_{bind} ranging from -63.1 kcal/mol for compound **1** to -75.7 kcal/mol for compounds **8** (GP44) and **11** (GP41). Furthermore, for the #site3 our calculation highlighted a docking score ranging from -6.22 kcal/mol for compound **2** (GP36) to -8.95 kcal/mol for compound **8**, while the ΔG_{bind} ranging from -72.6 kcal/mol for compound **2** to -85.2 kcal/mol for compound **8**.

The second step of our computational protocol consisted of evaluating the drug-like profile of compounds with favorable affinity, as found by molecular docking calculation. From this assessment, we selected only molecules having a drug-like profile more favorable than the one displayed by resveratrol. In fact, the identified compounds showed satisfactory LogP and solubility (LogS) along

with a good capacity to cross membranes, as suggested by the predicted values regarding the models of permeability (Caco-2 and MDCK cells). In fact, these values are abundantly over 500, indicating a strong ability to cross biological barriers (Table 1). Moreover, the potential SIRT1 activators were predicted to be devoid of cardiotoxicity. The assessment of oral absorption showed a favorable predicted profile for the identified compounds with respect to resveratrol. Furthermore, this assessment highlighted the scarce pharmacokinetic profile for resveratrol as largely reported in literature. Additionally, the evaluation of the physico-chemical features showed that the screened compounds are not pan-assay interference compounds (PAINS), although the output highlighted a low risk warning for compounds containing phenol and catechol moiety. In conclusion, our computational approaches provided eleven potential SIRT1 activators with favorable drug-like profile (Table 1).

Table 1. Final hits and their computational parameters derived from *in silico* studies.

Cpd	GlideScore (kcal/mol)	ΔG_{bind} (kcal/mol)	SASA[a]	QPlogP[b]	QPlogS[c]	QPPCaco[d]	QPPMDCK[e]	QPlogHERG[f]	%HOA[g]
1, GP14	#site1 -6.32 #site2 -6.43 #site3 -6.78	#site1 -81.6 #site2 -63.1 #site3 -73.5	459	2.43	-2.65	2512	1339	-5.46	100
2, GP36	#site1 -7.91 #site2 -6.45 #site3 -6.22	#site1 -86.3 #site2 -65.1 #site3 -72.6	590	5.23	-5.91	6867	3970	-6.67	100
3, GP35	#site1 -7.32 #site2 -6.18 #site3 -6.94	#site1 -86.8 #site2 -65.7 #site3 -79.5	661	5.39	-6.13	6868	3971	-6.46	100
4, GP42	#site1 -8.49 #site2 -6.41 #site3 -6.29	#site1 -94.7 #site2 -69.1 #site3 -75.7	589	5.22	-5.88	6866	3969	-6.65	100
5, GP32	#site1 -8.14 #site2 -7.36 #site3 -7.19	#site1 -88.3 #site2 -73.7 #site3 -74.2	565	4.39	-5.42	2083	1093	-6.63	89
6, GP37	#site1 -8.62 #site2 -6.31 #site3 -7.88	#site1 -86.5 #site2 -72.9 #site3 -81.6	588	2.57	-4.66	2423	2198	-6.40	85
7, GP46	#site1 -7.09 #site2 -6.22 #site3 -6.41	#site1 -84.2 #site2 -66.8 #site3 -75.6	665	5.35	-6.2	6889	3971	-6.49	100
8, GP44	#site1 -8.56 #site2 -6.91 #site3 -8.95	#site1 -106.3 #site2 -75.7 #site3 -85.2	590	2.82	-4.67	2910	1830	-6.38	90
9, GP30	#site1 -7.91 #site2 -6.81 #site3 -6.47	#site1 -93.8 #site2 -71.4 #site3 -75.2	688	6.027	-6.36	6881	3989	-7.16	91
10, GP27d	#site1 -8.44 #site2 -6.99 #site3 -6.83	#site1 -107.4 #site2 -72.7 #site3 -75.9	635	4.30	-5.74	2432	1301	-7.08	88
11, GP41	#site1 -7.00 #site2 -6.86 #site3 -6.92	#site1 -86.3 #site2 -75.7 #site3 -85.1	583	5.27	-5.77	8383	4925	-6.56	100
Rsv[h]	#site1 -7.12 #site2 -7.16 #site3 -7.21	#site1 -89.2 #site2 -64.7 #site3 -81.4	482	2.00	-2.81	279	123	-5.33	71

[a]SASA predicted the total solvent accessible surface (range or recommended value for 95% of known drugs 300 - 1000); [b]QPlogP predicted octanol/water partition coefficient (range or recommended value for 95% of known drugs -2 - 6.5); [c]QPlogS predicted aqueous solubility in mol/dm^3(range or recommended value for 95% of known drugs -6.5-0.5); [d]QPPCaco predicted apparent Caco-2 cell permeability in nm/sec (range or recommended value for 95% of known drugs >500 great); [e]QPPMDCK predicted apparent MDCK cell permeability in nm/sec (range or recommended value for 95% of known drugs >500 great); [f]QPlogHERG predicted IC_{50} values for blockage of HERG K^+ channels (range or recommended value for 95% of known drugs below -5); [g]h%HOA predicted human oral absorption on 0 to 100% scale (range or recommended value for 95% of known drugs >80% high). Range or recommended values are reported in QikProp user manual; [h]resveratrol.

Accordingly, applying the described *in silico* protocol, we identified drug-like compounds with computational scores comparable or even better with respect to the scores found for resveratrol. In Figure 2 is reported the docking output of compound **8**, that is one of the most promising screened compounds. Briefly, based on the computational output, this compound can strongly target all three binding sites on SIRT1, as highlighted by docking scores and relative ligand binding energies (compound **8**: #site1, GlideScore = -8.56 kcal/mol, and ΔG_{bind} = -106.3 kcal/mol; #site2, GlideScore = -6.91 kcal/mol, and ΔG_{bind} = -75.7 kcal/mol; #site3, GlideScore = -8.95 kcal/mol, and ΔG_{bind} = -85.2 kcal/mol. Resveratrol: #site1, GlideScore = -7.12 kcal/mol, and ΔG_{bind} = -89.2 kcal/mol; #site2, GlideScore = -7.16 kcal/mol, and ΔG_{bind} = -64.7 kcal/mol; #site3, GlideScore = -7.21 kcal/mol, and ΔG_{bind} = -81.4 kcal/mol) (Table 1). In particular, compound **8** into the #site1 establishes a H-bond with N226 and a relevant network of hydrophobic interactions with the residues in the binding site and with the p53-AMC-peptide. Regarding the #site2, compound **8** can target the sidechain of N226 and p53-AMC-peptide by establishing two H-bonds, in a similar fashion as resveratrol. Notably, in addition to the mentioned H-bonds, compound **8** establishes a polar contact with the backbone of E214. Hydrophobic contacts were observed and in particular we noted a π-π stacking with the aromatic moiety of p53-AMC-peptide. Finally, when docked into #site3, compound **8** can target, with its catechol moiety, D292 and D298 by two H-bonds. Also, a H-bond with the sidechain of E208 was observed (Figure 2). This pattern of interaction within SIRT1-binding sites accounted for a significant interaction with the enzyme, sharing a similar mechanism found for resveratrol. Accordingly, due to this similarity, compound **8** is identified as one of the most promising SIRT1 activators.

Lastly, to validate the computational approach, the identified potential SIRT1 activators (Figure 3) were synthesized and submitted to a biological evaluation.

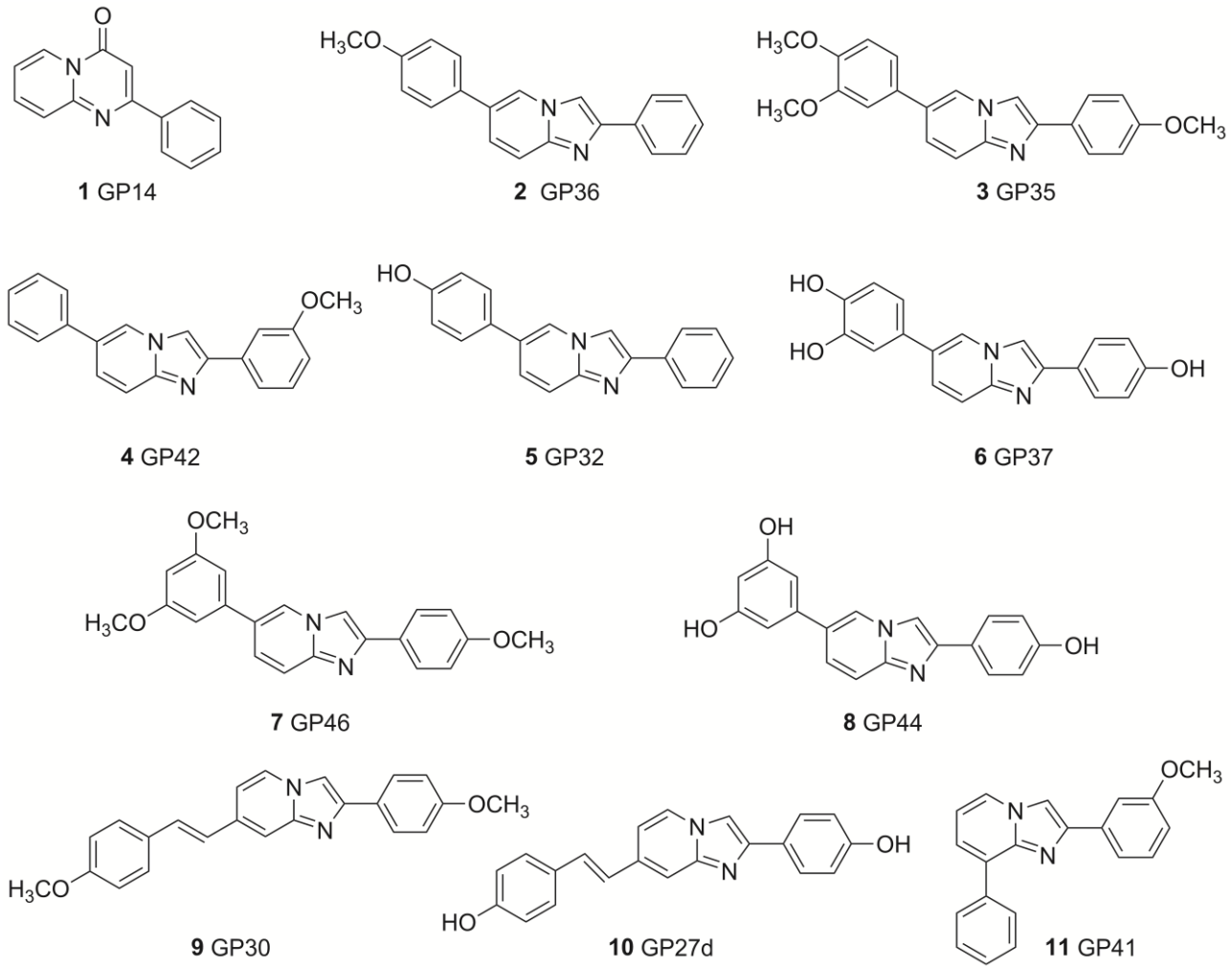

Figure 3. Chemical structures of potential SIRT1 activators.

2.2. Synthesis of selected hit compounds

Compound **1**, 2-phenyl-4*H*-pyrido[1,2-*a*]pyrimidin-4-one (Figure 3) was synthesized as previously described [59] by condensing 2-aminopyridine **12** with ethyl 3-oxo-3-phenylpropanoate, in the presence of polyphosphoric acid (PPA) at 100 °C (Scheme 1).

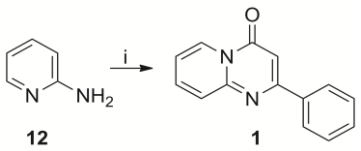

Scheme 1. Synthesis of 2-phenyl-4*H*-pyrido[1,2-*a*]pyrimidin-4-one **1**.

Reagents and conditions: (i) ethyl 3-oxo-3-phenylpropanoate, PPA, Δ.

Derivatives **2-6** (Figure 3), characterized by an imidazo[1,2-*a*]pyridine central core, were obtained as outlined in Scheme 2. Reaction of 2-amino-5-bromo pyridine **13** with the suitably substituted 2-bromo-1-phenylethan-1-one, in the presence of potassium carbonate, achieved the corresponding 2-phenyl-imidazo[1,2-*a*]pyridines **14a-c**, which were then coupled with differently substituted-phenylboronic acids under Suzuky-Miyaura conditions [61] to obtain the desired activators **2-4**. Treatment of the methoxy derivatives **2** and **3** with BBr_3 in a dichloromethane solution gave the corresponding hydroxy-substituted compounds **5** and **6**.

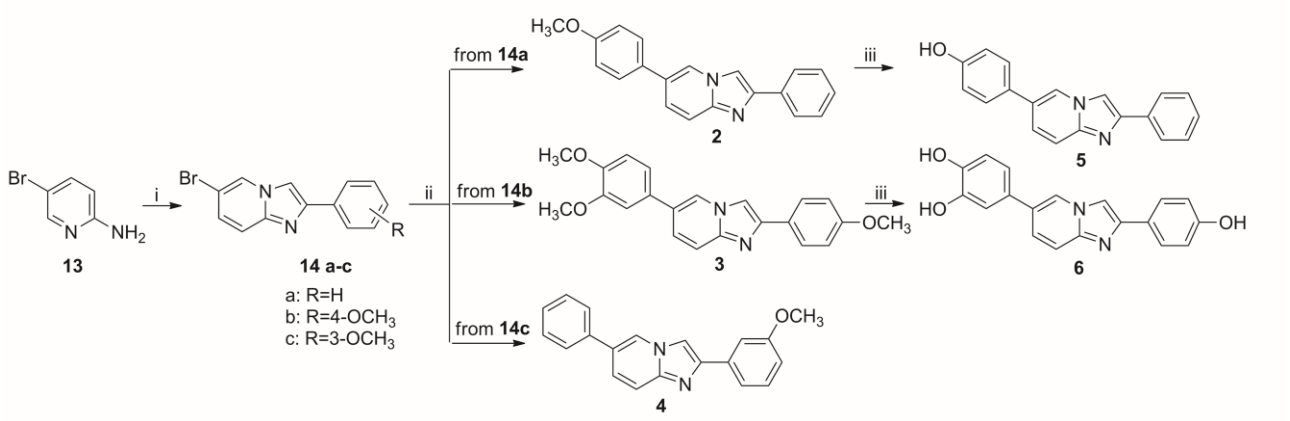

Scheme 2. Synthesis of imidazo[1,2-*a*]pyridine derivatives **2-6**.

Reagents and conditions: (i) 2-Bromo-1-(substituted)phenylethan-1-one, $NaHCO_3$, Δ; (ii) substituted-phenylboronic acid, $Pd(OAc)_2$, PPh_3, Na_2CO_3, Δ; (iii) BBr_3, CH_2Cl_2.

The imidazopyridines **7** and **8** (Figure 3) were synthesized according to the alternative synthetic sequence described in Scheme 3. A coupling reaction between 2-amino-5-bromopyridine **13** and 3,5-dimethoxyphenylboronic acid, under the standard conditions referenced above, gave the key intermediate 5-(3,5-dimethoxyphenyl)pyridin-2-amine **15**, which was cyclized to the imidazo[1,2-*a*]pyridine **7** by reaction with 2-bromo-1-(4-methoxyphenyl)ethan-1-one. The following ether cleavage, performed using BBr_3 in a dichloromethane solution, afforded the hydroxy-substituted activator **8**.

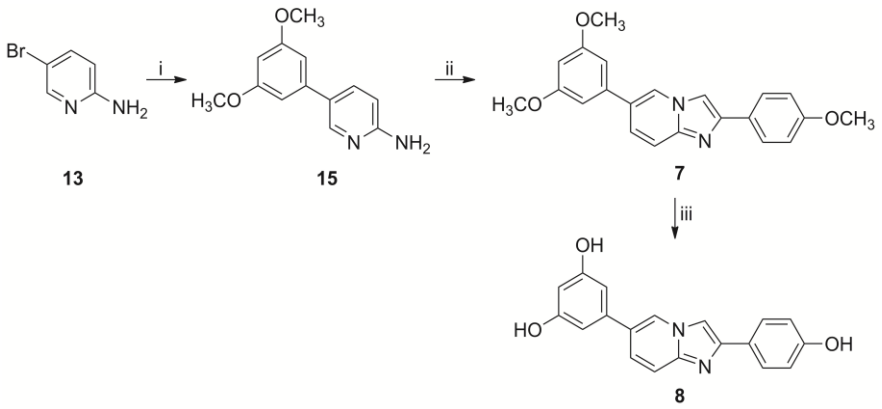

13 15 7 8

Scheme 3. Synthesis of imidazo[1,2-*a*]pyridine derivatives **7** and **8**.

Reagents and conditions: (i) 3,5-dimethoxyphenylboronic acid, $Pd(OAc)_2$, PPh_3, Na_2CO_3, Δ; (ii) 2-bromo-1-(4-methoxy)phenylethan-1-one, $NaHCO_3$, Δ; iii) BBr_3, CH_2Cl_2.

Compounds **9** and **10** (Figure 3), bearing a 7-styryl fragment, were obtained as illustrated in Scheme 4. Cyclization of the commercially accessible 4-bromopyridin-2-amine **16** to 7-bromo-2-(4-methoxyphenyl)imidazo[1,2-*a*]pyridine **17**, achieved upon reaction with 2-bromo-1-(4-methoxy)phenylethan-1-one, and the subsequent coupling of **17** with 1-methoxy-4-vinylbenzene under the Heck conditions [62], afforded the di-methoxy derivative **9**, which was converted into the corresponding di-hydroxy-substituted product **10** by reaction with BBr_3 in a dichloromethane solution.

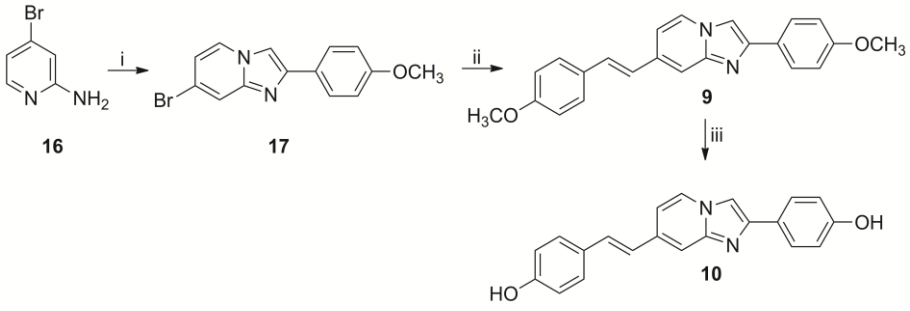

16 17 9 10

Scheme 4. Synthesis of imidazo[1,2-*a*]pyridine derivatives **9** and **10**.

Reagents and conditions: (i) 2-bromo-1-(4-methoxyphenyl)ethan-1-one, Δ; (ii) 1-methoxy-4-vinylbenzene, $Pd(OAc)_2$, PPh_3, Et_3N, DMF, Δ; (iii) BBr_3, CH_2Cl_2.

Derivative **11** (Figure 3), characterized by a pendant phenyl ring in position 8 of the imidazopyridine core, was obtained by a Suzuky-Miyaura coupling on the 8-bromo-2-(3-methoxyphenyl)imidazo[1,2-*a*]pyridine intermediate **18**, obtained in turn by cyclization of commercial 3-bromopyridin-2-amine **19** with 2-bromo-1-(3-methoxy)phenylethan-1-one in basic conditions (Scheme 5).

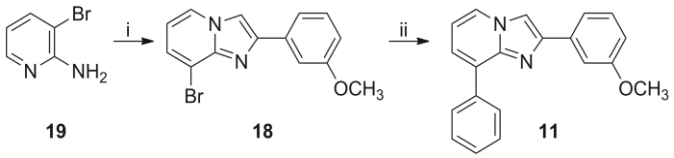

Scheme 5. Synthesis of 2-(3-methoxyphenyl)-8-phenylimidazo[1,2-*a*]pyridine **11**.

Reagents and conditions: (i) 2-bromo-1-(3-methoxyphenyl)ethan-1-one, Δ; (ii) 1-methoxy-4-vinylbenzene, $Pd(OAc)_2$, PPh_3, Δ.

2.3. In vitro evaluation of potential SIRT1 activators

The potential SIRT1 activators, identified by the computational approach, were tested using a SIRT1-specific enzymatic assay at a concentration of 100 μM, to compare their activity with the reference compound, resveratrol (Rsv, tested, according to literature, at 100 μM, Figure 4). Among the tested compounds, **4** (GP42), **6** (GP37), **8** (GP44), **9** (GP30), and **11** (GP41) showed significant stimulation of SIRT1 enzyme. Conversely, compounds **1** (GP14) and **5** (GP32) were unable to influence the activity of SIRT1 enzyme. Compounds **2** (GP36), **3** (GP35), **7** (GP46) and **10** (GP27d) were discontinued from the test due to the inconsistency of the results, precluding the reproducibility of the behavior of the compounds as SIRT1 activators.

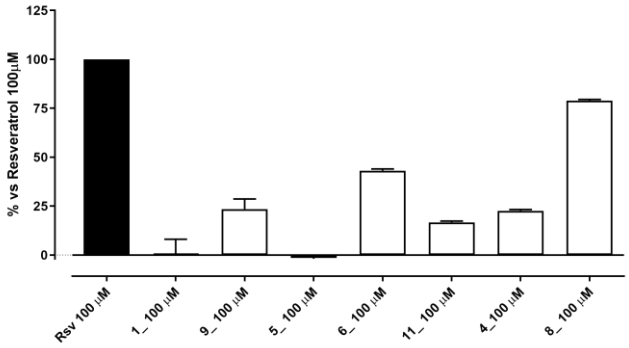

Figure 4. Stimulation of SIRT1 enzyme promoted by the selected compounds. SIRT1 activity is expressed as % *vs* the effect observed with Rsv 100 µM. The vertical bars symbolize the standard errors (n = 6).

In summary, based on the *in vitro* test on isolated enzyme, our screening protocol had a success rate of roughly 45% (hit rate) in identifying compounds behaving as SIRT1 activators, as five of eleven compounds showed significant activation of the enzyme.

Regarding the compounds endowed with stimulating properties, only compound **8** showed comparable potency to resveratrol, reaching at 100 µM an enzyme activity of 79 ± 1%. Furthermore, compound **8**, in the range from 1 to 300 µM, exhibited a perfect concentration-response curve (Figure 5), demonstrating to be an activator of SIRT1. Accordingly, compound **8** was further investigated in *ex vivo* experiments, to evaluate its cardioprotective properties.

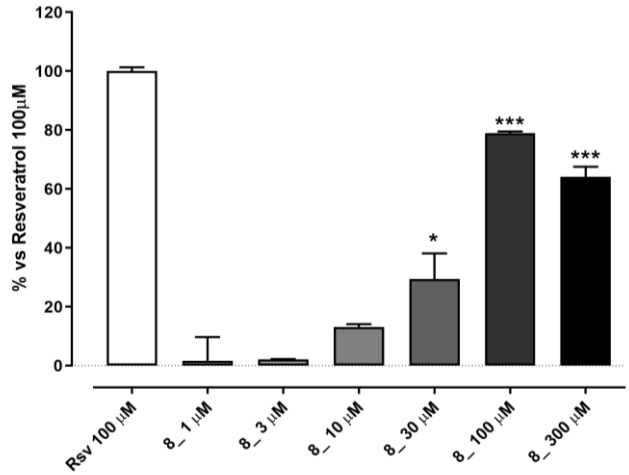

Figure 5. Concentration-response curve of SIRT1 enzyme activation mediated by compound **8**. SIRT1 activity is expressed as % *vs* the effect observed with Rsv 100 µM. The vertical bars symbolize

the standard errors (n = 6). Asterisks show a statistically significant difference from the value observed in the hearts of vehicle-treated animals (*P < 0.05; **P < 0.01; ***P < 0.005).

*2.4. Anti-ischemic activity of compound **8** in an ex vivo model of I/R*

The functional efficacy of compound **8** was investigated in a heart isolated and perfused on Langendorff apparatus submitted to I/R protocol, which represents a well-known model to reproduce myocardial damage induced by ischemic events. In our experimental conditions, an I/R episode produced marked damage to the isolated hearts of vehicle-treated rats. At this regard, a marked decrease of the functional parameters of myocardial contractile function (RPP) was observed during the reperfusion time and at the end the value of RPP was 29 ± 3%, compared to the pre-ischemic period (Figure 6A). Accordingly, in vehicle-treated hearts a wide and fast ischemic contracture was observed (MIC = 85 ± 18% and Thc = 18 ± 1 min, Figure 6B-C). The damage induced by the I/R event was also visible through morphometric analysis, and a size of ischemic area equal to 42 ± 2 % was measured using formazan salt (Figure 6D). Finally, the dosage of lactate dehydrogenase (LDH) levels in the perfusate, a well-known biochemical marker of myocardial injury, confirmed the compromise of cardiac function. LDH was abundantly released in the perfusate during the first part of reperfusion, according to the literature (Breschi et al., 2006) and the total amount at the end of reperfusion was 86 ± 9 U/g (Figure 6E).

Very interestingly, treatment with compound **8** (50 mg/kg) improved functional as well as morphometric and biochemical markers. Indeed, at the end of the reperfusion period the RPP value was significantly increased (53 ± 7%) and the typical ischemic contracture was later and reduced if compared to vehicle-treatment (MIC = 48 ± 17% and Thc = 24 ± 1 min, Figures 6A-C). The reduced impairment induced by I/R on the functional parameters of isolated hearts from compound **8**-treated animals was consistent with a significantly reduced degree of damage (Ai/A_{LV} % = 19 ± 5%, Figure 6D) and with the almost-halved amount of LDH released during the reperfusion period (40 ± 1 U/g,

Figure 6E). Taken together, these results unequivocally demonstrate the cardioprotective activity of compound **8** against I/R injury.

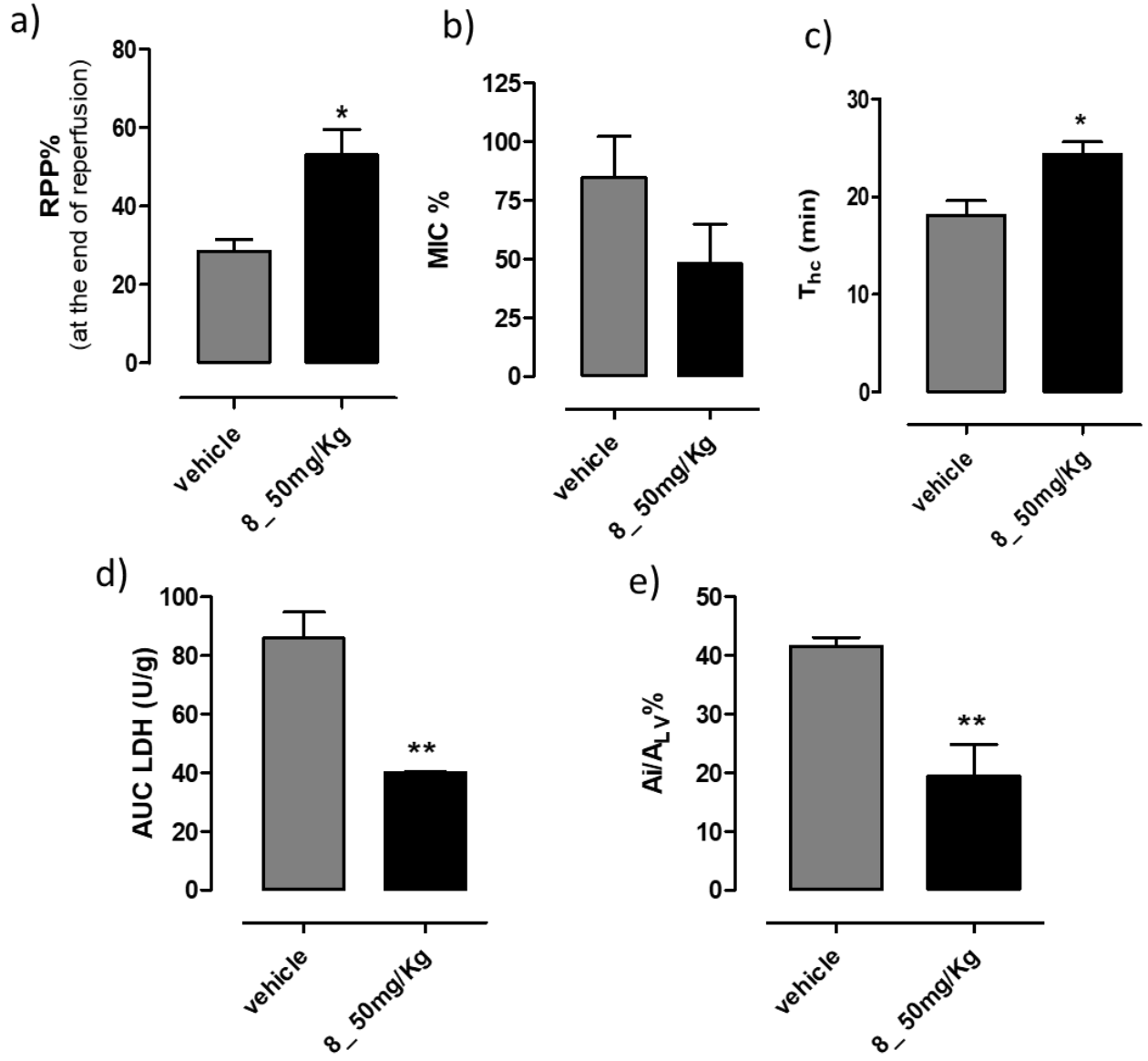

Figure 6. The histograms represent the functional, biochemical and morphological changes induced by treatment of the animals with compound **8** or with vehicle before I/R episode. **(A)** Changes in RPP% at the end of reperfusion; **(B)** Changes in the maximal ischemic contraction (MIC) expressed as % *vs* pre-ischemic inotropism; **(C)** Changes in the time of half-ischemic contracture (Thc) expressed as min; **(D)** Changes in LDH amount released in the reperfusion period (U/g); **(E)** Changes in the percentage of ischemic area *vs* left ventricle area (Ai/A_{LV} %). The vertical bars symbolize the

standard errors (n = 6). Asterisks show a statistically significant difference from the value observed in the hearts of vehicle-treated animals (*P < 0.05; **P < 0.01).

3. Conclusions

In summary, in this work we described the development of an integrated screening platform, enclosing computational, medicinal chemistry, and pharmacological competencies, for the identification of SIRT1 activators and their preliminary pharmacological validation as cardioprotective agents. Starting from an in-house library containing synthetic molecules inspired by nature, including both bioisosters of natural flavonoids and rigidified and constrained analogs of resveratrol, we developed a computational screening protocol employing the crystal structure of SIRT1 enzyme and the mentioned library, to identify a small set of potential SIRT1 activators. To validate our computational approach, the retrieved eleven compounds were synthesized in appropriate amount and submitted to *in vitro* studies for evaluating their capacity to activate SIRT1 enzyme. Among the tested compounds, five of them were found able to activate SIRT1 enzyme and one of them (compound **8**, GP44) was selected for further characterization due to the superior response in activating the enzyme and its favorable calculated drug-like profile. Compound **8** was employed in *ex vivo* studies for a preliminary evaluation of its pharmacological profile.

This study clearly confirms a close link between the activation of SIRT1 and cardioprotection, identifying the SIRT1 activator compound **8** as the most promising cardioprotective agent of the screened compounds. This pharmacological tool paves the way for developing innovative cardioprotective agents able to target this epigenetic drug target.

4. Materials and Methods

4.1. Computational details

4.1.1. Database and protein preparation

The in-house library of chemical compounds was built using tools available in Maestro software (Maestro release 2018, Schrödinger, LLC, New York, NY, 2018). This library, for a total of 54 compounds, includes both pyrido[1,2-*a*]pyrimidine derivatives, developed as bioisosters of flavonoids, and imidazo[1,2-*a*]pyridine compounds, designed as rigidified and constrained analogs of the natural product resveratrol. All structures, generated in the previous step, were minimized employing MacroModel program (MacroModel release 2018, Schrödinger, LLC, New York, NY, 2018) adopting the force field OPLS3 [63]. For simulating the solvent effects, the GB/SA model was employed, selecting ‘‘no cutoff’’ for non-bonded interactions. The PRCG technique (5000 maximum iterations and threshold for gradient convergence = 0.001) was employed. The resulting structures were treated by LigPrep software (LigPrep release 2018, Schrödinger, LLC, New York, NY, 2018) for identifying the most probable ionization state at cellular pH value (7.4 ± 0.5).

The three-dimensional structure of the human SIRT1 enzyme was obtained from the Protein Data Bank (PDB ID 5BTR [46]; crystal structure of SIRT1 in complex with resveratrol and an AMC-containing peptide) and imported into Maestro suite 2018 and prepared by means of protein preparation wizard protocol for obtaining a suitable starting structure for further computational experiments [13, 64]. Using this protocol, we performed a series of computational steps to (1) add hydrogens, (2) optimize the orientation of hydroxyl groups, Asn, and Gln, and the protonation state of His, and (3) perform a constrained minimization refinement using the *impref* utility. In particular, at first, the protein was preprocessed by adding all hydrogen atoms to structure, assigning bond orders, creating disulfide bonds and filling missing side chains and loops. To optimize the hydrogen bond network, His tautomers and ionization states were predicted, 180° rotations of the terminal angle of Asn, Gln, and His residues were assigned, and hydrogen atoms of the hydroxyl and thiol groups

were sampled. Finally, a restrained minimization was performed using the Impact Refinement (*impref*) module, employing OPLS3 force field to optimize the geometry and minimize the energy of the protein. The minimization was terminated when the energy converged, or the RMSD reached a maximum cutoff of 0.30 Å.

4.1.2. Virtual screening

The library, prepared as described, was screened against SIRT1 enzyme using Glide software (Glide release 2018, Schrödinger, LLC, New York, NY, 2018) with XP-scoring function as previously performed by us [52]. Due to the mechanism of activation described for resveratrol and highlighted by the crystal structure in which resveratrol is bound to SIRT1 in three binding sites; we prepared the energy grids for docking, using the default value of the protein atom-scaling factor (1.0 Å), with a cubic box centered on crystallized resveratrol molecules. In this way, we prepared a specific grid for each binding site found for resveratrol. After the generation of the grids, the library of compounds was docked into SIRT1, considering the three binding sites of resveratrol. The docked poses considered for the post-docking minimization step were 1000, evaluating the Glide XP docking score. Notably, the XP technique was capable of correctly accommodating the resveratrol into three distinct binding sites (Figure S1). In particular, the calculation of the root-mean-square deviation (RMSD), performed using the tool available in Maestro suite, showed a lower value between the crystallized structure and the docked pose of resveratrol for each selected binding site (#site1, RMSD 0.148 Å; #site2, RMSD 0.143 Å; #site3, RMSD 0.151 Å). This procedure is a well-established technique for validating the docking protocol employed in virtual screening campaigns [65-69].

For improving the quality of the screening, we also evaluated the ligand binding energies from the complexes derived by the docking calculation. For this purpose, Prime/MM-GBSA method available in Prime software (Prime release 2018, Schrödinger, LLC, New York, NY, 2018). This technique computes the variation between the free and the complex state of both the ligand and enzyme after energy minimization [70, 71].

4.1.2. Evaluation of drug-like profile

The drug-like profile was assessed *in silico* employing QikProp application (QikProp release 2018, Schrödinger, LLC, New York, NY, 2018). Pan Assay Interference Compounds (PAINS) assessment was executed employing FAFDrugs4 web-server [60] (https://fafdrugs4.rpbs.univ-paris-diderot.fr/ access date February 2021) as previously reported [72]. In particular, regarding the calculation performed by Qikprop, QPPCaco (model for the gut-blood barrier) predicts apparent Caco-2 cell permeability in nm/sec, while QPPMDCK (model for the for the blood brain barrier) predicts apparent MDCK cell permeability in nm/sec. Remarkably, QikProp predictions are for non-active transport.

4.2. Chemistry

Melting points were determined using a Reichert Köfler hot-stage apparatus and are uncorrected. Routine ^{1}H-NMR and ^{13}C-NMR spectra were recorded in DMSO-d6 solution on a Bruker 400 spectrometer operating at 400 MHz. Evaporation was done *in vacuo* (rotary evaporator). Analytical TLCs were conducted on Merck 0.2 mm precoated silica gel aluminum sheets (60 F-254). Purity of compounds was determined by HPLC analysis, using a Shimadzu LC-20AD liquid chromatograph (PDA, 250−500 nm) and a Luna C18 column (250 mm × 4.6 mm, 5 μm, Phenomenex), with a gradient of either water and acetonitrile (compounds **1-5**,**9**,**11**) or water, acetonitrile and acetic acid (compounds **6**,**8**,**10**) and a flow rate of 1.0 mL/min. All the compounds showed percent purity values ≥ 95%. Pyridin-2-amine, 3-bromopyridin-2-amine, 4-bromopyridin-2-amine, 5-bromopyridin-2-amine, ethyl 3-oxo-3-phenylpropanoate, 2-bromo-1-phenylethan-1-one 2-bromo-1-(3-methoxyphenyl)ethan-1-one, 2-bromo-1-(4-methoxyphenyl)ethan-1-one, 1-methoxy-4-vinyl benzene, and suitably substituted-phenylboronic acids used to obtain the target compounds were from Aldrich and Activate Scientific.

2-Phenyl-4*H*-pyrido[1,2-*a*]pyrimidin-4-one **1** [59], 6-Bromo-2-phenylimidazo[1,2-*a*]pyridine **14a** [73], 6-bromo-2-(4-methoxyphenyl)imidazo[1,2-*a*]pyridine **14b** [73], 6-bromo-2-(3-

methoxyphenyl)imidazo[1,2-*a*]pyridine **14c** [73], 8-bromo-2-(3-methoxyphenyl)imidazo[1,2-*a*]-pyridine **18** [74] were synthesized following the described procedures.

4.2.1. General Procedure for the Synthesis of 2,6-(Substituted)diphenylimidazo[1,2-a]pyridines (***2-4***)

A solution of the appropriate 6-bromoimidazo[1,2-*a*]pyridine derivative **14a-c** (1.00 mmol), $Pd(OAc)_2$ (0.10 mmol) and PPh_3 (0.20 mmol) in toluene was added with the suitable phenylboronic acid (1.50 mmol), dissolved in ethanol, and 2 mL of Na_2CO_3 2 M. The resulting mixture was refluxed under stirring until the disappearance of the starting material (TLC analysis). After cooling, the crude obtained were evaporated to dryness and the residue was extracted (water/ethyl acetate) and purified by column chromatography (silica gel, eluting system ethyl acetate/petroleum ether). The pure product was recrystallized from the suitable solvent then characterized by the physico-chemical and spectroscopic data.

*4.2.2. 6-(4-methoxyphenyl)-2-phenylimidazo[1,2-a]pyridine (**2**)*

M.p. 157-161 °C. Cryst. Solvent: Acetonitrile. Yield: 70%. ^{1}H-NMR (δ, ppm): 8.765 (s, 1H); 8.369 (s, 1H); 7.944 (d, J = 7.81 Hz, 2H); 7.653-7.609 (m, 4H); 7.444 (t, J = 6.84 Hz, 1H); 7.342 (d, J = 6.35 Hz, 2H); 7.047 (d, J = 7.32 Hz, 2H), 3.985 (s, 3H). ^{13}C-NMR (δ, ppm): 159.56; 145.14; 144.42; 134.27; 129.37; 129.20; 128.15; 126.03; 125.52; 123.63; 116.96; 115.03; 109.92.

*4.2.3. 6-(3,4-dimethoxyphenyl)-2-(4-methoxyphenyl)imidazo[1,2-a]pyridine (**3**).*

M.p. 141-144 °C. Cryst. Solvent: Acetonitrile. Yield: 49%. ^{1}H-NMR (δ, ppm): 8.805 (s, 1H); 8.259 (s, 1H); 7.906 (d, J = 8.79 Hz, 2H); 7.624-7.588 (m, 3H); 7.284-7.218 (m, 2H); 7.034 (t, J = 8.54 Hz, 3H); 3.865 (s, 3H); 3.796 (s, 6H). ^{13}C-NMR (δ, ppm): 159.52; 149.67; 149.12; 145.37; 144.45; 129.83; 127.34; 126.99; 125.53; 125.26; 123.63; 119.16; 116.64; 114.62; 112.74; 110.74; 108.75; 56.12; 55.60.

*4.2.4. 2-(3-methoxyphenyl)-6-phenylimidazo[1,2-a]pyridine (**4**)*

M.p. 139-141 °C. Cryst. Solvent: Acetonitrile. Yield: 39%. ^{1}H-NMR (δ, ppm): 8.877 (s, 1H); 8.433 (s, 1H); 7.741 (d, J = 7.24 Hz, 2H); 7.690 (d, J = 9.36 Hz, 1H); 7.618 (dd, J_1 = 9.36 Hz, J_2 = 1.76 Hz, 1H); 7.565-7.570 (m, 2H); 7.522 (t, J = 7.44 Hz, 2H); 7.418-7.403 (m, 1H); 7.370 (t, J = 8.20 Hz, 1H); 6.912 (dd, J_1 = 7.91 Hz, J_2 = 1.76 Hz, 1H); 3.845 (s, 3H). ^{13}C-NMR (δ, ppm): 160.13; 145.25; 144.54; 137.12; 135.72; 130.29; 129.58; 128.20; 127.00; 125.72; 125.46; 124.45; 118.46; 117.13; 114.11; 111.11; 110.32; 55.56.

*4.2.5. General Procedure for the Synthesis of 4-(2-phenylimidazo[1,2-a]pyridin-6-yl)phenol (**5**) and 4-(2-(4-methoxyphenyl)imidazo[1,2-a]pyridin-6-yl)benzene-1,2-diol (**6**)*

A solution of the appropriate methoxy derivative, **2** and **3** (1.00 mmol), in CH_2Cl_2 anhydrous was cooled at -10 °C, then added with BBr_3 (1.50 mmol) and left under stirring at room temperature until the disappearance of the starting material (TLC analysis). The resulting suspension was then carefully poured into crushed ice and the solid precipitated was collected by filtration, recrystallized from the suitable solvent and characterized by the physico-chemical and spectroscopic data.

*4.2.6. 4-(2-phenylimidazo[1,2-a]pyridin-6-yl)phenol (**5**)*

M.p. > 230 °C. Cryst. Solvent: Methanol. Yield: 44%. ^{1}H-NMR (δ, ppm): 9.896 (s, 1H, exc.); 9.161 (s, 1H); 8.766 (s, 1H); 8.230 (d, J = 10.0 Hz, 1H); 7.992 (d, J = 8.40 Hz, 3H); 7.653-7.541 (m, 5H); 6.962 (d, J = 8.40 Hz, 2H). ^{13}C-NMR (δ, ppm): 158.85; 139.56; 136.27; 133.10; 130.86; 130.42; 129.98; 128.74; 127.00; 126.67; 125.60; 125.16; 116.66; 112.47; 111.75.

*4.2.7. 4-(2-(4-hydroxyphenyl)imidazo[1,2-a]pyridin-6-yl)benzene-1,2-diol (**6**)*

M.p. > 230 °C. Cryst. Solvent: 2-propanol. Yield: 23%. ^{1}H-NMR (δ, ppm): 10.164 (s, 1H, exc.); 9.469 (s, 1H, exc.); 9.259 (s, 1H, exc.); 9.029 (s, 1H); 8.526 (s, 1H); 8.106 (d, J = 9.60 Hz, 1H); 7.905 (d, J = 9.20 Hz, 1H); 7.793 (d, J = 8.80 Hz, 2H); 7.143 (d, J = 2.40 Hz, 1H); 7.072 (dd, J_1 = 8.00 Hz, J_2 = 2.20 Hz, 1H); 6.987 (d, J = 8.40 Hz, 2H); 6.916 (d, J = 8.40 Hz, 1H). ^{13}C-NMR (δ, ppm): 159.91; 146.96; 146.56; 139.33; 130.47; 129.92; 128.36; 126.29; 124.93; 118.65; 116.79; 116.73; 114.61; 112.27; 110.02.

*4.2.8. Synthesis of 6-(3,5-dimethoxyphenyl)-2-(4-methoxyphenyl)imidazo[1,2-a]pyridine (**7**)*

A mixture of 5-(3,5-dimethoxyphenyl)pyridin-2-amine **15** (1.00 mmol), 2-bromo-1-(4-methoxyphenyl)ethan-1-one (1.00 mmol) and $NaHCO_3$ (1.20 mmol) was refluxed under stirring at 100 °C until the disappearance of the starting material (TLC analysis). After cooling, the crude obtained were evaporated to dryness; water was then added to the residue and the desired heterocycle, **7**, separated as a white solid, was collected by filtration, purified by recrystallization from ethanol, and characterized with physico-chemical and spectroscopic data. M.p. 140-142 °C. Yield: 34%. ^{1}H-NMR (δ, ppm): 8.879 (s, 1H); 8.272 (s, 1H); 7.910 (d, J = 8.80 Hz, 2H); 7.597 (t, J = 3.60 Hz, 2H); 7.015 (d, J = 8.80 Hz, 2H); 6.860 (d, J = 2.00 Hz, 2H); 6.530 (t, J = 4.40 Hz, 1H); 3.824 (s, 6H); 3.798 (s, 3H).

*4.2.9. Synthesis of 5-(2-(4-hydroxyphenyl)imidazo[1,2-a]pyridin-6-yl)benzene-1,3-diol (**8**)*

A solution of 6-(3,5-dimethoxyphenyl)-2-(4-methoxyphenyl)imidazo[1,2-*a*]pyridine **7** (1.00 mmol) in anhydrous CH_2Cl_2 was cooled at -10 °C and added with BBr_3 (3.20 mmol). The resulting mixture was then left under stirring at room temperature until the disappearance of the starting material (TLC analysis). At the end, it was carefully poured into crushed ice and the solid precipitated was collected by filtration, recrystallized from *i*PrOH and characterized by the physico-chemical and spectroscopic data. M.p. 259-262 °C. Yield: 35%. ^{1}H-NMR (δ, ppm): 10.086 (s, 1H, exc.); 9.588 (s, 2H, exc.); 9.043 (s, 1H); 8.507 (s, 1H); 8.028 (d, J = 8.00 Hz, 1H); 7.889 (d, J = 9.20 Hz, 1H); 7.791 (d, J = 8.80Hz, 2H); 6.978 (d, J = 8.80 Hz, 2H); 6.575 (d, J = 2.40 Hz, 2H); 6.365 (s, 1H). ^{13}C-NMR (δ, ppm): 159.93; 159.68; 139.78; 137.14; 132.44; 130.39; 128.39; 125.97; 116.74; 112.41; 110.12; 105.57; 103.37.

*4.2.10. Synthesis of 5-(3,5-dimethoxyphenyl)pyridin-2-amine (**15**)*

A solution of 5-bromopyridin-2-amine **13** (1.00 mmol), $Pd(OAc)_2$ (0.10 mmol) and PPh_3 (0.20 mmol) in ethanol and water (3:1) was added with (3,5-dimethoxyphenyl)boronic acid (1.50 mmol) and Na_2CO_3 (1.5 mmol). The resulting mixture was refluxed under stirring at 110 °C until the

disappearance of the starting material (TLC analysis). After cooling, the crude obtained were evaporated to dryness and the residue was washed with water and extracted with ethyl acetate, then purified by column chromatography (silica gel, eluting system ethyl acetate/petroleum ether) obtaining an oily product. The pure product was then characterized by physico-chemical and spectroscopic data. Yield: 82%. ^{1}H-NMR (δ, ppm): 8.278 (d, J = 2.00 Hz, 1H); 7.724 (dd, J_1 = 8.80 Hz, J_2 = 2.80 Hz, 1H); 6.717 (d, J = 2.00 Hz, 2H); 6.530 (d, J = 8.80 Hz, 1H); 6.433 (t, J = 4.40 Hz, 1H); 6.106 (s, 2H, exc.); 3.812 (s, 6H).

*4.2.11. Synthesis of 7-bromo-2-(4-methoxyphenyl)imidazo[1,2-a]pyridine (**17**)*

A mixture of 4-bromopyridin-2-amine **16** (1.00 mmol) and 2-bromo-1-(4-methoxyphenyl)ethan-1-one (1.00 mmol) was heated at 80 °C for 8 h, until the disappearance of the starting material (TLC analysis). The crude obtained were purified through recrystallization from methanol and characterized with physico-chemical and spectroscopic data. M.p. 290-295 °C. Yield: 77%. ^{1}H-NMR (δ, ppm): 8.75 (d, 1H); 8.433 (s, 1H); 7.991 (s, 1H); 7.845 (d, J = 8.8 Hz, 2H); 7.344 (dd, J_1 = 2.00 Hz, J_2 = 1.60 Hz, 1H); 7.074 (d, J = 8.8 Hz, 2H); 3.806 (s, 3H).

*4.2.12. Synthesis of (E)-2-(4-methoxyphenyl)-7-(4-methoxystyryl)imidazo[1,2-a]pyridine (**9**)*

A mixture of 7-bromo-2-(4-methoxyphenyl)imidazo[1,2-*a*]pyridine **17**, (10.0 mmol), PPh_3 (0.70 mmol) and $Pd(OAc)_2$ (0.30 mmol) was added with 1-methoxy-4-vinylbenzene (20.0 mmol), Et_3N (20.0 mmol) and DMF, then heated under stirring at 100 °C for 18 h until the disappearance of the starting material (TLC analysis). After cooling, the crude obtained were evaporated to dryness, washed with water, purified through recrystallization from methanol and characterized with physico-chemical and spectroscopic data. M.p. 267-270 °C. Yield: 48%. ^{1}H-NMR (δ, ppm): 8.454 (d, J = 7.2 0 Hz, 1H); 8.251 (s, 1H); 7.897 (d, J = 8.80 Hz, 2H); 7.588 (d, J = 8.40 Hz, 3H); 7.330 (d, J = 16.40 Hz, 1H); 7.256 (d, J = 7.20 Hz, 1H); 7.174 (d, J = 16.40 Hz, 1H); 7.029-6.977 (m, 4H); 3.806 (d, J = 3.20 Hz, 6H). ^{13}C-NMR (δ, ppm): 159.81; 159.70; 145.66; 145.35; 145.07; 132.36; 130.55; 129.77; 128.59; 127.46; 127.38; 115.90; 114.75; 114.67; 114.40; 109.01; 108.93; 55.62.

*4.2.13. Synthesis of (E)-4-(2-(2-(4-hydroxyphenyl)imidazo[1,2-a]pyridin-7-yl)vinyl)phenol (**10**)*

A solution of the methoxy derivative **9** (1.00 mmol) in CH_2Cl_2 anhydrous was cooled at -10 °C and added with BBr_3 (2.00 mmol). The resulting mixture was then left under stirring at room temperature until the disappearance of the starting material (TLC analysis). At the end, it was carefully poured into crushed ice and the solid precipitated was collected by filtration, recrystallized from methanol and characterized by the physico-chemical and spectroscopic data. M.p. > 230 °C. Yield: 28%. ^{1}H-NMR (δ, ppm): 10.122 (s,1H, exc.); 9.89 (s, 1H, exc.); 8.741 (d, J = 5.60 Hz, 1H); 8.50 (s, 1H); 7.779-7.729 (m, 4H); 7.652-7.548 (m, 3H); 7.314 (d, J = 15.20 Hz, 1H); 6.971 (d, J = 8.40 Hz, 2H); 6.847 (d, J = 8.40 Hz, 2H). ^{13}C-NMR (δ, ppm): 159.25; 158.91; 145.66; 145.35; 144.87; 132.77; 130.55; 129.08; 128.15; 127.73; 125.84; 116.82; 116.68; 115.90; 114.40; 109.01; 108.93.

*4.2.14. Synthesis of 2-(3-methoxyphenyl)-8-phenylimidazo[1,2-a]pyridine (**11**)*

A solution of 8-bromo-2-(3-methoxyphenyl)imidazo[1,2-*a*]pyridine **18** (1.00 mmol), $Pd(OAc)_2$ (0.10 mmol) and PPh_3 (0.20 mmol) in toluene was added with phenyl boronic acid (1.50 mmol), dissolved in ethanol, and 2 mL of Na_2CO_3 2 M. The resulting mixture was refluxed under stirring until the disappearance of the starting material (TLC analysis). After cooling, the crude obtained were evaporated to dryness and the residue was extracted (water/ethyl acetate) and purified by column chromatography (silica gel, eluting system ethyl acetate/petroleum ether) obtaining an oily product. The pure product was then characterized by the physico-chemical and spectroscopic data. Yield: 49%. ^{1}H-NMR (δ, ppm): 8.544 (dd, J_1 = 6.70 Hz, J_2 = 1.00 Hz, 1H); 8.522 (s, 1H); 8.220 (d, J = 7.20 Hz, 2H); 7.560-7.508 (m, 4H); 7.498 (dd, J_1 = 7.10 Hz, J_2 = 1.10 Hz, 1H); 7.460-7.412 (m ,1H); 7.377 (t, J = 7.80 Hz, 1H); 7.020 (t, J = 6.90 Hz, 1H); 6.917 (dd, J_1 = 7.80 Hz, J_2 = 2.60 Hz, 1H); 3.834 (s, 3H). ^{13}C-NMR (δ, ppm): 160.09; 144.61; 143.74; 136.60; 135.74; 130.28; 129.12; 128.77; 128.59; 126.58; 123.49; 118.58; 113.61; 113.05; 111.66; 110.49; 55.55.

4.3. In vitro assay

SIRT1 activity was measured using a SIRT1 direct fluorescent screening assay kit (Cayman, Ann Arbor, MI), following the manufacturer's protocol. Before performing the test, the possible interferences of the compounds under examination with the fluorophore and/or developer were evaluated according to manufacturer's protocol. Compounds with an interference % to the fluorophore and developer less than or equal to 10% were considered suitable. Briefly, 25 μL of Assay Buffer, 5 μL of SIRT1 human recombinant appropriately reconstituted and diluted and 5 μL of the test compounds suitably solubilized in DMSO (10^{-2} M) and diluted in bidistilled water, were added to the three wells. 30 μL of Assay Buffer and 5 μL of solvent used to solubilize the compounds under examination (DMSO) were plated to three wells (background). 25 μL of Assay Buffer, 5 μL of SIRT1 and 5 μL of reference activator (resveratrol) were plated to three wells.

The final concentration in the wells of the tested compounds and resveratrol was 100 μM and 1% v/v for DMSO. Compound **8** was also tested at 300 μM, 30 μM, 10 μM, 3 μM, 1 μM concentrations. The fluorescence intensity was monitored with EnSpire® (2300 Multilabel Reader, PerkinElmer) by setting an excitation wavelength of 350 nm and an emission wavelength of 450 nm. The fluorescence values referred to the blank were subtracted, and the data were normalized considering the vehicle fluorescence value as 0% activity and the value recorded with the fluorescence emitted in the presence of resveratrol 100 μM as 100%.

4.3.1. Data analysis

All values are expressed as a mean ± standard error for three different experiments in duplicate.

The effects of SIRT1 activator compounds were statistically analyzed by one-way ANOVA followed by Bonferroni post-test. $P < 0.05$ was considered indicative of a significant difference.

4.4. Ex vivo studies

All procedures were performed according to European (EEC Directive 2010/63) and Italian (D.L. March 4, 2014 n. 26) legislation (protocol number 45972, 21/09/2016). Animals were housed in cages with food and water ad libitum, and exposed to 12 h:12 h light/dark cycles.

Adult male Wistar rats, 300–350 g, were treated with an intraperitoneal injection of compound **8** (50 mg/kg) or vehicle (dimethyl sulfoxide; DMSO). The dosage of compound **8** was established according to the dosage of resveratrol in studies in which cardioprotective effects were evaluated [75-78].

After 2 h, the rats were anaesthetised with sodium pentobarbital (100 mg/kg, i.p.) and heparinised (100 U, i.p.) to prevent blood clotting. Subsequently, the hearts were quickly excised, mounted on a Langendorff apparatus and perfused at constant pressure (70-80 mmHg), as previously published [76-80]. To check the functional parameters of the heart, a latex balloon filled with bidistilled water at a pressure of 5-10 mmHg was inserted into the left ventricle through the mitral valve and connected to a pressure transducer (Bentley Trantec, mod 800, Ugo Basile, Comerio, Italy) and in turn, to a data acquisition system (Byopac, California USA). The functional parameter of rate pressure product (RPP) was calculated as RPP = HR x LVDP, where HR was the heart rate value and LVDP was the left ventricular developed pressure, continuously monitored by a computerised Byopac system (Goleta, CA, USA). After 30 min of equilibration, the hearts were submitted to 30 min of global ischemia. During this period, a typical ischemic contracture was observed, thus the amplitude of the maximal ischemic contracture (MIC) was expressed as a percentage of pre-ischemic LVDP; while the time required to reach a half-maximal ischemic contracture (Thc) was measured in min. At the end of the ischemic period the hearts were re-perfused for 120 min and RPP value was acquired at intervals of 10 min. Before ischemia and during reperfusion, the perfusate was collected to evaluate the enzyme LDH. In particular, LDH, a biochemical marker of ischemic damage, was measured by spectrophotometric method in the perfusate collected in the last 5 min of the pre-ischemic phase and then every 5 min during the first 30 min of reperfusion, and every 10 min in the remaining period of

reperfusion. LDH was assessed by adding 27.6 mM pyruvate and 4.8 mM NADH, and measuring the conversion of NADH to NAD^+ at λ= 340 nm, in kinetics for 2.5 min. The amount of released LDH has been expressed in U/g in 120 min of reperfusion, resulting from the AUC analysis (area under the curve of the LDH amount recorded) and related to 1 g of the heart weight.

At the end of reperfusion, the hearts were removed from the apparatus, dried, weighed and subsequently the left ventricle was isolated. This was cut in slices of about 2 mm, which were immersed in a 1% w/v solution of 2,3,5 triphenyltetrazolium chloride (TTC, Sigma-Aldrich) dissolved in a phosphate buffer (pH = 7.4) for 20 min in the dark and at 37 °C. TTC reacts with dehydrogenases present in intact and viable cells, and oxidizes to formazan, a red and insoluble compound. Then, slices were fixed in a water solution of formaldehyde 10% v/v. Subsequently, the ventricular slices were photographed and analyzed to identify the necrotic areas (visible as a white or light pink color) and the healthy areas (visible as a strong red due to the TTC reaction). It was possible to calculate the ischemic area as a percentage of the total area of the left ventricle, through photographs of the sections subjected to planimetric analysis carried out 24 h after the reaction with the TTC (Ai/A_{LV}).

4.4.1. Data analysis

All values are expressed as a mean ± standard error for six different experiments.

The effects of compound **8** on RPP, MIC, Thc, Ai/A_{LV} and LDH were statistically analyzed by Student's t-test. $P < 0.05$ was considered indicative of a significant difference.

Acknowledgments

This work is supported by the Università di Pisa under the "PRA – Progetti di Ricerca di Ateneo" (Institutional Research Grants) – Project no PRA_2020_58 "Agenti innovativi e nanosistemi per target molecolari nell'ambito dell'oncologia di precisione" to Simone Brogi.

References

[1] J. Rine, J.N. Strathern, J.B. Hicks, I. Herskowitz, A suppressor of mating-type locus mutations in Saccharomyces cerevisiae: evidence for and identification of cryptic mating-type loci, Genetics, 93 (1979) 877-901.
[2] S.Y. Park, J.S. Kim, A short guide to histone deacetylases including recent progress on class II enzymes, Exp Mol Med, 52 (2020) 204-212.
[3] P. Martinez-Redondo, A. Vaquero, The diversity of histone versus nonhistone sirtuin substrates, Genes Cancer, 4 (2013) 148-163.
[4] P. Gallinari, S.D. Marco, P. Jones, M. Pallaoro, C. Steinkühler, HDACs, histone deacetylation and gene transcription: from molecular biology to cancer therapeutics, Cell Res, 17 (2007) 195-211.
[5] R.A. Frye, Phylogenetic classification of prokaryotic and eukaryotic Sir2-like proteins, Biochem Biophys Res Commun, 273 (2000) 793-798.
[6] I.V. Gregoretti, Y.M. Lee, H.V. Goodson, Molecular evolution of the histone deacetylase family: functional implications of phylogenetic analysis, J Mol Biol, 338 (2004) 17-31.
[7] M. Haberland, R.L. Montgomery, E.N. Olson, The many roles of histone deacetylases in development and physiology: implications for disease and therapy, Nat Rev Genet, 10 (2009) 32-42.
[8] V. Carafa, A. Nebbioso, L. Altucci, Sirtuins and Disease: The Road Ahead, Front Pharmacol, 3 (2012).
[9] M.C. Haigis, D.A. Sinclair, Mammalian Sirtuins: Biological Insights and Disease Relevance, Annu Rev Pathol, 5 (2010) 253-295.
[10] R.H. Houtkooper, E. Pirinen, J. Auwerx, Sirtuins as regulators of metabolism and healthspan, Nat Rev Mol Cell Biol, 13 (2012) 225-238.
[11] M. Brindisi, A.P. Saraswati, S. Brogi, S. Gemma, S. Butini, G. Campiani, Old but Gold: Tracking the New Guise of Histone Deacetylase 6 (HDAC6) Enzyme as a Biomarker and Therapeutic Target in Rare Diseases, J Med Chem, 63 (2019) 23-39.
[12] E. Landucci, M. Brindisi, L. Bianciardi, L.M. Catania, S. Daga, S. Croci, E. Frullanti, C. Fallerini, S. Butini, S. Brogi, S. Furini, R. Melani, A. Molinaro, F.C. Lorenzetti, V. Imperatore, S. Amabile, J. Mariani, F. Mari, F. Ariani, T. Pizzorusso, A.M. Pinto, F.M. Vaccarino, A. Renieri, G. Campiani, I. Meloni, iPSC-derived neurons profiling reveals GABAergic circuit disruption and acetylated alpha-tubulin defect which improves after iHDAC6 treatment in Rett syndrome, Exp Cell Res, 368 (2018) 225-235.
[13] M. Brindisi, J. Senger, C. Cavella, A. Grillo, G. Chemi, S. Gemma, D.M. Cucinella, S. Lamponi, F. Sarno, C. Iside, A. Nebbioso, E. Novellino, T.B. Shaik, C. Romier, D. Herp, M. Jung, S. Butini, G. Campiani, L. Altucci, S. Brogi, Novel spiroindoline HDAC inhibitors: Synthesis, molecular modelling and biological studies, Eur J Med Chem, 157 (2018) 127-138.
[14] M. Dokmanovic, C. Clarke, P.A. Marks, Histone Deacetylase Inhibitors: Overview and Perspectives, Mol Cancer Res, 5 (2007) 981-989.
[15] A. Kumar, S. Chauhan, How much successful are the medicinal chemists in modulation of SIRT1: A critical review, Eur J Med Chem, 119 (2016) 45-69.
[16] V. Carafa, D. Rotili, M. Forgione, F. Cuomo, E. Serretiello, G.S. Hailu, E. Jarho, M. Lahtela-Kakkonen, A. Mai, L. Altucci, Sirtuin functions and modulation: from chemistry to the clinic, Clin Epigenetics, 8 (2016) 61.
[17] S. Michan, D. Sinclair, Sirtuins in mammals: insights into their biological function, Biochem J, 404 (2007) 1-13.
[18] M. Tanno, J. Sakamoto, T. Miura, K. Shimamoto, Y. Horio, Nucleocytoplasmic shuttling of the NAD+-dependent histone deacetylase SIRT1, J Biol Chem, 282 (2007) 6823-6832.
[19] E. Verdin, M.D. Hirschey, L.W. Finley, M.C. Haigis, Sirtuin regulation of mitochondria: energy production, apoptosis, and signaling, Trends Biochem Sci, 35 (2010) 669-675.
[20] R. Mostoslavsky, K.F. Chua, D.B. Lombard, W.W. Pang, M.R. Fischer, L. Gellon, P. Liu, G. Mostoslavsky, S. Franco, M.M. Murphy, K.D. Mills, P. Patel, J.T. Hsu, A.L. Hong, E. Ford, H.L. Cheng, C. Kennedy, N. Nunez, R. Bronson, D. Frendewey, W. Auerbach, D. Valenzuela, M. Karow, M.O. Hottiger, S. Hursting, J.C. Barrett, L. Guarente, R. Mulligan, B. Demple, G.D. Yancopoulos, F.W. Alt, Genomic instability and aging-like phenotype in the absence of mammalian SIRT6, Cell, 124 (2006) 315-329.
[21] T. Nakagawa, L. Guarente, Sirtuins at a glance, J Cell Sci, 124 (2011) 833-838.
[22] M.C. Haigis, L.P. Guarente, Mammalian sirtuins--emerging roles in physiology, aging, and calorie restriction, Genes Dev, 20 (2006) 2913-2921.

[23] B.J. North, B.L. Marshall, M.T. Borra, J.M. Denu, E. Verdin, The Human Sir2 Ortholog, SIRT2, Is an NAD+-Dependent Tubulin Deacetylase, Mol Cell, 11 (2003) 437-444.
[24] P. Oberdoerffer, S. Michan, M. McVay, R. Mostoslavsky, J. Vann, S.K. Park, A. Hartlerode, J. Stegmuller, A. Hafner, P. Loerch, S.M. Wright, K.D. Mills, A. Bonni, B.A. Yankner, R. Scully, T.A. Prolla, F.W. Alt, D.A. Sinclair, SIRT1 redistribution on chromatin promotes genomic stability but alters gene expression during aging, Cell, 135 (2008) 907-918.
[25] R.H. Wang, K. Sengupta, C. Li, H.S. Kim, L. Cao, C. Xiao, S. Kim, X. Xu, Y. Zheng, B. Chilton, R. Jia, Z.M. Zheng, E. Appella, X.W. Wang, T. Ried, C.X. Deng, Impaired DNA damage response, genome instability, and tumorigenesis in SIRT1 mutant mice, Cancer Cell, 14 (2008) 312-323.
[26] L. Bosch-Presegue, A. Vaquero, Sirtuin-dependent epigenetic regulation in the maintenance of genome integrity, FEBS J, 282 (2015) 1745-1767.
[27] M. Potente, L. Ghaeni, D. Baldessari, R. Mostoslavsky, L. Rossig, F. Dequiedt, J. Haendeler, M. Mione, E. Dejana, F.W. Alt, A.M. Zeiher, S. Dimmeler, SIRT1 controls endothelial angiogenic functions during vascular growth, Genes Dev, 21 (2007) 2644-2658.
[28] S. Winnik, J. Auwerx, D.A. Sinclair, C.M. Matter, Protective effects of sirtuins in cardiovascular diseases: from bench to bedside, Eur Heart J, 36 (2015) 3404-3412.
[29] T. Liu, P.Y. Liu, G.M. Marshall, The critical role of the class III histone deacetylase SIRT1 in cancer, Cancer Res, 69 (2009) 1702-1705.
[30] S. Caito, S. Rajendrasozhan, S. Cook, S. Chung, H. Yao, A.E. Friedman, P.S. Brookes, I. Rahman, SIRT1 is a redox-sensitive deacetylase that is post-translationally modified by oxidants and carbonyl stress, FASEB J, 24 (2010) 3145-3159.
[31] T.T. Schug, Q. Xu, H. Gao, A. Peres-da-Silva, D.W. Draper, M.B. Fessler, A. Purushotham, X. Li, Myeloid deletion of SIRT1 induces inflammatory signaling in response to environmental stress, Mol Cell Biol, 30 (2010) 4712-4721.
[32] F. Ng, L. Wijaya, B.L. Tang, SIRT1 in the brain-connections with aging-associated disorders and lifespan, Front Cell Neurosci, 9 (2015) 64.
[33] A.S. Banks, N. Kon, C. Knight, M. Matsumoto, R. Gutierrez-Juarez, L. Rossetti, W. Gu, D. Accili, SirT1 gain of function increases energy efficiency and prevents diabetes in mice, Cell Metab, 8 (2008) 333-341.
[34] M. Kitada, S. Kume, A. Takeda-Watanabe, K. Kanasaki, D. Koya, Sirtuins and renal diseases: relationship with aging and diabetic nephropathy, Clin Sci (Lond), 124 (2013) 153-164.
[35] H.G. Budayeva, E.A. Rowland, I.M. Cristea, Intricate Roles of Mammalian Sirtuins in Defense against Viral Pathogens, J Virol, 90 (2016) 5-8.
[36] C. Tatone, G. Di Emidio, M. Vitti, M. Di Carlo, S. Santini, Jr., A.M. D'Alessandro, S. Falone, F. Amicarelli, Sirtuin Functions in Female Fertility: Possible Role in Oxidative Stress and Aging, Oxid Med Cell Longev, 2015 (2015) 659687.
[37] H.T. Chung, Y. Joe, Antagonistic crosstalk between SIRT1, PARP-1, and -2 in the regulation of chronic inflammation associated with aging and metabolic diseases, Integr Med Res, 3 (2014) 198-203.
[38] D. Kim, M.D. Nguyen, M.M. Dobbin, A. Fischer, F. Sananbenesi, J.T. Rodgers, I. Delalle, J.A. Baur, G. Sui, S.M. Armour, P. Puigserver, D.A. Sinclair, L.H. Tsai, SIRT1 deacetylase protects against neurodegeneration in models for Alzheimer's disease and amyotrophic lateral sclerosis, EMBO J, 26 (2007) 3169-3179.
[39] L. Gan, L. Mucke, Paths of convergence: sirtuins in aging and neurodegeneration, Neuron, 58 (2008) 10-14.
[40] J. Hu, H. Jing, H. Lin, Sirtuin inhibitors as anticancer agents, Future Med Chem, 6 (2014) 945-966.
[41] B.P. Hubbard, D.A. Sinclair, Small molecule SIRT1 activators for the treatment of aging and age-related diseases, Trends Pharmacol Sci, 35 (2014) 146-154.
[42] N. Chaudhary, P.T. Pfluger, Metabolic benefits from Sirt1 and Sirt1 activators, Curr Opin Clin Nutr Metab Care, 12 (2009) 431-437.
[43] X. Li, Y. Feng, X.X. Wang, D. Truong, Y.C. Wu, The Critical Role of SIRT1 in Parkinson's Disease: Mechanism and Therapeutic Considerations, Aging Dis, 11 (2020) 1608-1622.
[44] G. Donmez, T.F. Outeiro, SIRT1 and SIRT2: emerging targets in neurodegeneration, EMBO Mol Med, 5 (2013) 344-352.
[45] Z.Z. Chong, S. Wang, Y.C. Shang, K. Maiese, Targeting cardiovascular disease with novel SIRT1 pathways, Future Cardiol, 8 (2012) 89-100.

[46] D. Cao, M. Wang, X. Qiu, D. Liu, H. Jiang, N. Yang, R.M. Xu, Structural basis for allosteric, substrate-dependent stimulation of SIRT1 activity by resveratrol, Genes Dev, 29 (2015) 1316-1325.
[47] S. Ma, J. Feng, R. Zhang, J. Chen, D. Han, X. Li, B. Yang, X. Li, M. Fan, C. Li, Z. Tian, Y. Wang, F. Cao, SIRT1 Activation by Resveratrol Alleviates Cardiac Dysfunction via Mitochondrial Regulation in Diabetic Cardiomyopathy Mice, Oxid Med Cell Longev, 2017 (2017) 4602715.
[48] X. Ma, Z. Sun, X. Han, S. Li, X. Jiang, S. Chen, J. Zhang, H. Lu, Neuroprotective Effect of Resveratrol via Activation of Sirt1 Signaling in a Rat Model of Combined Diabetes and Alzheimer's Disease, Front Neurosci, 13 (2019) 1400.
[49] B. Karaman Mayack, W. Sippl, F. Ntie-Kang, Natural Products as Modulators of Sirtuins, Molecules, 25 (2020).
[50] C. Iside, M. Scafuro, A. Nebbioso, L. Altucci, SIRT1 Activation by Natural Phytochemicals: An Overview, Front Pharmacol, 11 (2020) 1225.
[51] Y. Wang, X. Liang, Y. Chen, X. Zhao, Screening SIRT1 Activators from Medicinal Plants as Bioactive Compounds against Oxidative Damage in Mitochondrial Function, Oxid Med Cell Longev, 2016 (2016) 4206392.
[52] L. Testai, E. Piragine, I. Piano, L. Flori, E. Da Pozzo, V. Miragliotta, A. Pirone, V. Citi, L. Di Cesare Mannelli, S. Brogi, S. Carpi, A. Martelli, P. Nieri, C. Martini, C. Ghelardini, C. Gargini, V. Calderone, The Citrus Flavonoid Naringenin Protects the Myocardium from Ageing-Dependent Dysfunction: Potential Role of SIRT1, Oxid Med Cell Longev, 2020 (2020) 4650207.
[53] Q. Huang, H. Su, B. Qi, Y. Wang, K. Yan, X. Wang, X. Li, D. Zhao, A SIRT1 Activator, Ginsenoside Rc, Promotes Energy Metabolism in Cardiomyocytes and Neurons, J Am Chem Soc, 143 (2021) 1416-1427.
[54] K. de Vries, M. Strydom, V. Steenkamp, Bioavailability of resveratrol: Possibilities for enhancement, J Herb Med, 11 (2018) 71-77.
[55] L. Scisciola, F. Sarno, V. Carafa, S. Cosconati, S. Di Maro, L. Ciuffreda, A. De Angelis, P. Stiuso, A. Feoli, G. Sbardella, L. Altucci, A. Nebbioso, Two novel SIRT1 activators, SCIC2 and SCIC2.1, enhance SIRT1-mediated effects in stress response and senescence, Epigenetics, 15 (2020) 664-683.
[56] Y. An, C. Meng, Q. Chen, J. Gao, Discovery of small molecule sirt1 activator using high-throughput virtual screening, molecular dynamics simulation, molecular mechanics generalized born/surface area (MM/GBSA) calculation, and biological evaluation, Med Chem Res, 29 (2019) 255-261.
[57] V.K. Pulla, M. Alvala, D.S. Sriram, S. Viswanadha, D. Sriram, P. Yogeeswari, Structure-based drug design of small molecule SIRT1 modulators to treat cancer and metabolic disorders, J Mol Graph Model, 52 (2014) 46-56.
[58] H. Dai, D.A. Sinclair, J.L. Ellis, C. Steegborn, Sirtuin activators and inhibitors: Promises, achievements, and challenges, Pharmacol Ther, 188 (2018) 140-154.
[59] C. La Motta, S. Sartini, L. Mugnaini, F. Simorini, S. Taliani, S. Salerno, A.M. Marini, F. Da Settimo, A. Lavecchia, E. Novellino, M. Cantore, P. Failli, M. Ciuffi, Pyrido[1,2-a]pyrimidin-4-one derivatives as a novel class of selective aldose reductase inhibitors exhibiting antioxidant activity, J Med Chem, 50 (2007) 4917-4927.
[60] D. Lagorce, O. Sperandio, J.B. Baell, M.A. Miteva, B.O. Villoutreix, FAF-Drugs3: a web server for compound property calculation and chemical library design, Nucleic Acids Res, 43 (2015) W200-207.
[61] D. Blakemore, Synthetic Methods in Drug Discovery: Volume 1 Chapter 1. Suzuki-Miyaura Coupling, 1 (2016) 1-69.
[62] R.F. Heck, Palladium-Catalyzed Vinylation of Organic Halides. In Organic Reactions, (Ed.), (2005) 345-390.
[63] W.L. Jorgensen, D.S. Maxwell, J. Tirado-Rives, Development and Testing of the OPLS All-Atom Force Field on Conformational Energetics and Properties of Organic Liquids, J Am Chem Soc, 118 (1996) 11225-11236.
[64] A. Di Capua, C. Sticozzi, S. Brogi, M. Brindisi, A. Cappelli, L. Sautebin, A. Rossi, S. Pace, C. Ghelardini, L. Di Cesare Mannelli, G. Valacchi, G. Giorgi, A. Giordani, G. Poce, M. Biava, M. Anzini, Synthesis and biological evaluation of fluorinated 1,5-diarylpyrrole-3-alkoxyethyl ether derivatives as selective COX-2 inhibitors endowed with anti-inflammatory activity, Eur J Med Chem, 109 (2016) 99-106.
[65] A.M.S. Mascarenhas, R.B.M. de Almeida, M.F. de Araujo Neto, G.O. Mendes, J.N. da Cruz, C.B.R. Dos Santos, M.B. Botura, F.H.A. Leite, Pharmacophore-based virtual screening and molecular docking to identify promising dual inhibitors of human acetylcholinesterase and butyrylcholinesterase, J Biomol Struct Dyn, (2020) 1-10.

[66] C.B.R. Santos, K.L.B. Santos, J.N. Cruz, F.H.A. Leite, R.S. Borges, C.A. Taft, J.M. Campos, C. Silva, Molecular modeling approaches of selective adenosine receptor type 2A agonists as potential anti-inflammatory drugs, J Biomol Struct Dyn, 39 (2021) 3115-3127.
[67] R.P. Leao, J.V. Cruz, G.V. da Costa, J.N. Cruz, E.F.B. Ferreira, R.C. Silva, L.R. de Lima, R.S. Borges, G.B. Dos Santos, C.B.R. Santos, Identification of New Rofecoxib-Based Cyclooxygenase-2 Inhibitors: A Bioinformatics Approach, Pharmaceuticals (Basel), 13 (2020).
[68] P.H.F. Araujo, R.S. Ramos, J.N. da Cruz, S.G. Silva, E.F.B. Ferreira, L.R. de Lima, W.J.C. Macedo, J.M. Espejo-Roman, J.M. Campos, C.B.R. Santos, Identification of Potential COX-2 Inhibitors for the Treatment of Inflammatory Diseases Using Molecular Modeling Approaches, Molecules, 25 (2020).
[69] R.A.M. Neto, C.B.R. Santos, S.V.C. Henriques, L.O. Machado, J.N. Cruz, C. da Silva, L.B. Federico, E.H.C. Oliveira, M.P.C. de Souza, P.N.B. da Silva, C.A. Taft, I.M. Ferreira, M.R.F. Gomes, Novel chalcones derivatives with potential antineoplastic activity investigated by docking and molecular dynamics simulations, J Biomol Struct Dyn, (2020) 1-13.
[70] S. Brogi, M. Brindisi, S. Butini, G.U. Kshirsagar, S. Maramai, G. Chemi, S. Gemma, G. Campiani, E. Novellino, P. Fiorenzani, J. Pinassi, A.M. Aloisi, M. Gynther, R. Venskutonyte, L. Han, K. Frydenvang, J.S. Kastrup, D.S. Pickering, (S)-2-Amino-3-(5-methyl-3-hydroxyisoxazol-4-yl)propanoic Acid (AMPA) and Kainate Receptor Ligands: Further Exploration of Bioisosteric Replacements and Structural and Biological Investigation, J Med Chem, 61 (2018) 2124-2130.
[71] K. Frydenvang, D.S. Pickering, G.U. Kshirsagar, G. Chemi, S. Gemma, D. Sprogoe, A.M. Kaern, S. Brogi, G. Campiani, S. Butini, J.S. Kastrup, Ionotropic Glutamate Receptor GluA2 in Complex with Bicyclic Pyrimidinedione-Based Compounds: When Small Compound Modifications Have Distinct Effects on Binding Interactions, ACS Chem Neurosci, 11 (2020) 1791-1800.
[72] L. Zaccagnini, S. Brogi, M. Brindisi, S. Gemma, G. Chemi, G. Legname, G. Campiani, S. Butini, Identification of novel fluorescent probes preventing PrP(Sc) replication in prion diseases, Eur J Med Chem, 127 (2017) 859-873.
[73] L. Quattrini, E.L.M. Gelardi, V. Coviello, S. Sartini, D.M. Ferraris, M. Mori, I. Nakano, S. Garavaglia, C. La Motta, Imidazo[1,2-a]pyridine Derivatives as Aldehyde Dehydrogenase Inhibitors: Novel Chemotypes to Target Glioblastoma Stem Cells, J Med Chem, 63 (2020) 4603-4616.
[74] L. Quattrini, E.L.M. Gelardi, G. Petrarolo, G. Colombo, D.M. Ferraris, F. Picarazzi, M. Rizzi, S. Garavaglia, C. La Motta, Progress in the Field of Aldehyde Dehydrogenase Inhibitors: Novel Imidazo[1,2-a]pyridines against the 1A Family, ACS Med Chem Lett, 11 (2020) 963-970.
[75] L. Testai, A. Martelli, A. Marino, V. D'Antongiovanni, F. Ciregia, L. Giusti, A. Lucacchini, S. Chericoni, M.C. Breschi, V. Calderone, The activation of mitochondrial BK potassium channels contributes to the protective effects of naringenin against myocardial ischemia/reperfusion injury, Biochem Pharmacol, 85 (2013) 1634-1643.
[76] V. Calderone, L. Testai, A. Martelli, S. Rapposelli, M. Digiacomo, A. Balsamo, M.C. Breschi, Anti-ischemic properties of a new spiro-cyclic benzopyran activator of the cardiac mito-KATP channel, Biochem Pharmacol, 79 (2010) 39-47.
[77] L. Testai, E. Da Pozzo, I. Piano, L. Pistelli, C. Gargini, M.C. Breschi, A. Braca, C. Martini, A. Martelli, V. Calderone, The Citrus Flavanone Naringenin Produces Cardioprotective Effects in Hearts from 1 Year Old Rat, through Activation of mitoBK Channels, Front Pharmacol, 8 (2017) 71.
[78] L. Testai, A. Martelli, M. Cristofaro, M.C. Breschi, V. Calderone, Cardioprotective effects of different flavonoids against myocardial ischaemia/reperfusion injury in Langendorff-perfused rat hearts, J Pharm Pharmacol, 65 (2013) 750-756.
[79] V. Calderone, L. Testai, A. Martelli, C. La Motta, S. Sartini, F. Da Settimo, M.C. Breschi, Anti-ischaemic activity of an antioxidant aldose reductase inhibitor on diabetic and non-diabetic rat hearts, J Pharm Pharmacol, 62 (2010) 107-113.
[80] L. Testai, I. Strobykina, V.V. Semenov, M. Semenova, E.D. Pozzo, A. Martelli, V. Citi, C. Martini, M.C. Breschi, V.E. Kataev, V. Calderone, Mitochondriotropic and Cardioprotective Effects of Triphenylphosphonium-Conjugated Derivatives of the Diterpenoid Isosteviol, Int J Mol Sci, 18 (2017).

CRediT Author Statement for the manuscript PHASCI-D-21-00589

"Identification of Novel SIRT1 Activators Endowed with Cardioprotective Profile"

Lorenzo Flori: Investigation, Methodology, Formal Analysis, Validation **Giovanni Petrarolo:** Investigation, Methodology, Formal Analysis, Validation ***Simone Brogi*:** Conceptualization, Investigation, Methodology, Data curation, Software, Formal Analysis, Validation, Writing- Original draft preparation, Writing- Reviewing and Editing, Supervision **Concettina La Motta:** Conceptualization, Investigation, Methodology, Formal Analysis, Validation, Writing- Reviewing and Editing, Supervision **Lara Testai:** Conceptualization, Investigation, Methodology, Formal Analysis, Validation, Writing- Reviewing and Editing, Supervision **Vincenzo Calderone:** Data curation, Formal Analysis, Validation, Writing- Reviewing and Editing